Measurement of thermal transport coefficients at the nanoscale using ultrafast optical thermometry

David Cahill
Department of Materials Science and Engineering,
Materials Research Laboratory,
University of Illinois at Urbana-Champaign

Special thanks to Joe Feser, Judith Kimling, Johannes Kimling, Jun Liu, Rich Wilson, Xu Xie, Jonglo Park, Gyung-Min Choi, Hyejin Jang, and Kexin Yang

ILLINOIS

Outline

- Thermal transport coefficients and their length-scales and time-scales
- Time-domain thermoreflectance (TDTR)
  - experimental details and data acquisition
  - data analysis
  - sensitivities and error propagation
- Alternatives to metal thermoreflectance for probing temperature on fast time scales
  - magneto-optic Kerr effect and magnetic birefringence (magnetic materials and polarization of light)
  - the spin-dependent Seebeck effect and detection of spin currents
  - plasmonic resonance and transient absorption

Linear transport coefficients for heat: thermal conductance (W/K) per unit length, per unit area, and per unit volume

- Bulk heat currents, e.g., heat diffusion equation, Fourier's law in steady-state, governed by **thermal conductivity** Λ

$$J_Q = -\Lambda \nabla T \qquad \Lambda \propto \mathrm{W\ m^{-1}\ K^{-1}}$$

- Interface heat currents controlled by the **interface thermal conductance** *G*

$$J_Q = G \Delta T \qquad G \propto \mathrm{W\ m^{-2}\ K^{-1}}$$

- Volumetric heat currents exchanged between excitation, e.g., two-temperature model of electrons and magnons, **electron-phonon coupling parameter**

$$j_Q = g_{em}(T_e - T_m) \quad g_{em} \propto \mathrm{W\ m^{-3}\ K^{-1}}$$

Typical TDTR measurement geometry and thermal parameters

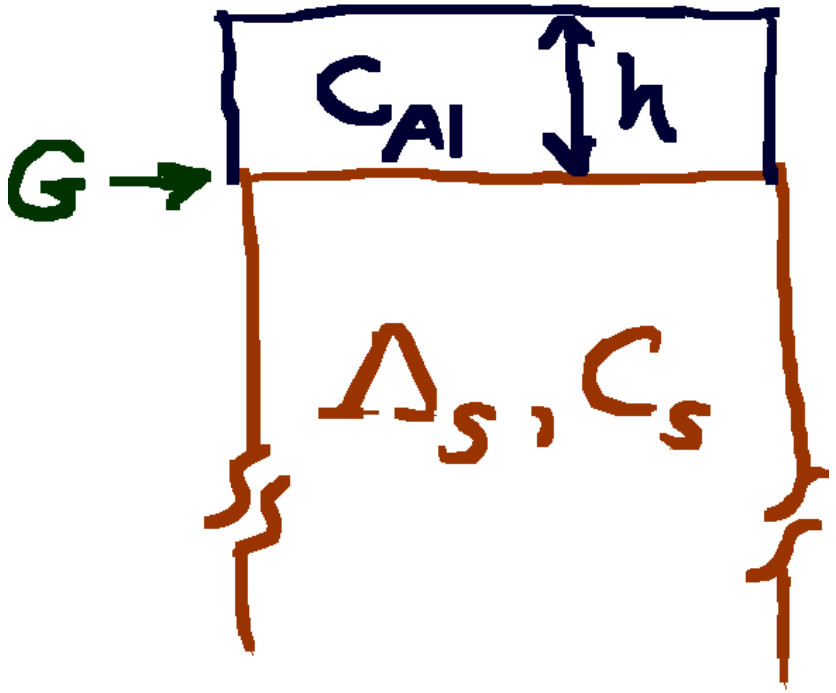

Kapitza length $L_K = \frac{\Lambda}{G}$

Length scale associated with thermal conductivity and electron-phonon coupling parameter

$$L_{ep} = \sqrt{\frac{\Lambda}{g_{ep}}}$$

$$3\ \text{nm} < L_{ep} < 100\ \text{nm}$$

Length and time scale

- Range of Kaptiza lengths
  - Al/diamond L_K ~ 10 μm
  - Al/polymer L_K ~ 1 nm

- Typical thickness for an opaque metal film is h=50 nm.
- Time scales $\tau_D = \frac{h^2}{D}$ for heat diffusion over a length scale of 50 nm
  - diamond $\tau_D \approx 25$ ps
  - polymer $\tau_D \approx 25$ ns

Length and time scale

- Typical “RC” time-constant for the thermal relaxation of a 50 nm metal film with cooling limited by an interface with G = 100 MW m^{-2} K^{-1}

$$\tau_G = \frac{hC}{G} = 1.5 \text{ ns}$$

Interesting to ask: What thermal conductivity gives

$$\tau_G = \tau_D \text{ , equivalent to } \quad h = L_K$$

$$\Lambda = 5 \text{ W m}^{-1} \text{ K}^{-1}$$

This provides a dividing line between “low” and “high” thermal conductivity in TDTR experiments

Length and time scale

- Bottom line:
  - ✓ to measure G we want to access time scales ~τ_G, typically ns.
  - ✓ to measure Λ we ideally access time scales > τ_D
- Modulated time-domain thermoreflectance gives us a way to access a wide range of time scales, from ps to

$$\tau_f = \frac{1}{2\pi f}, \text{ where } f \text{ is the modulation frequency}$$

- Typically f=10 MHz, so τ_f = 16 ns

Time-domain thermoreflectance (TDTR)

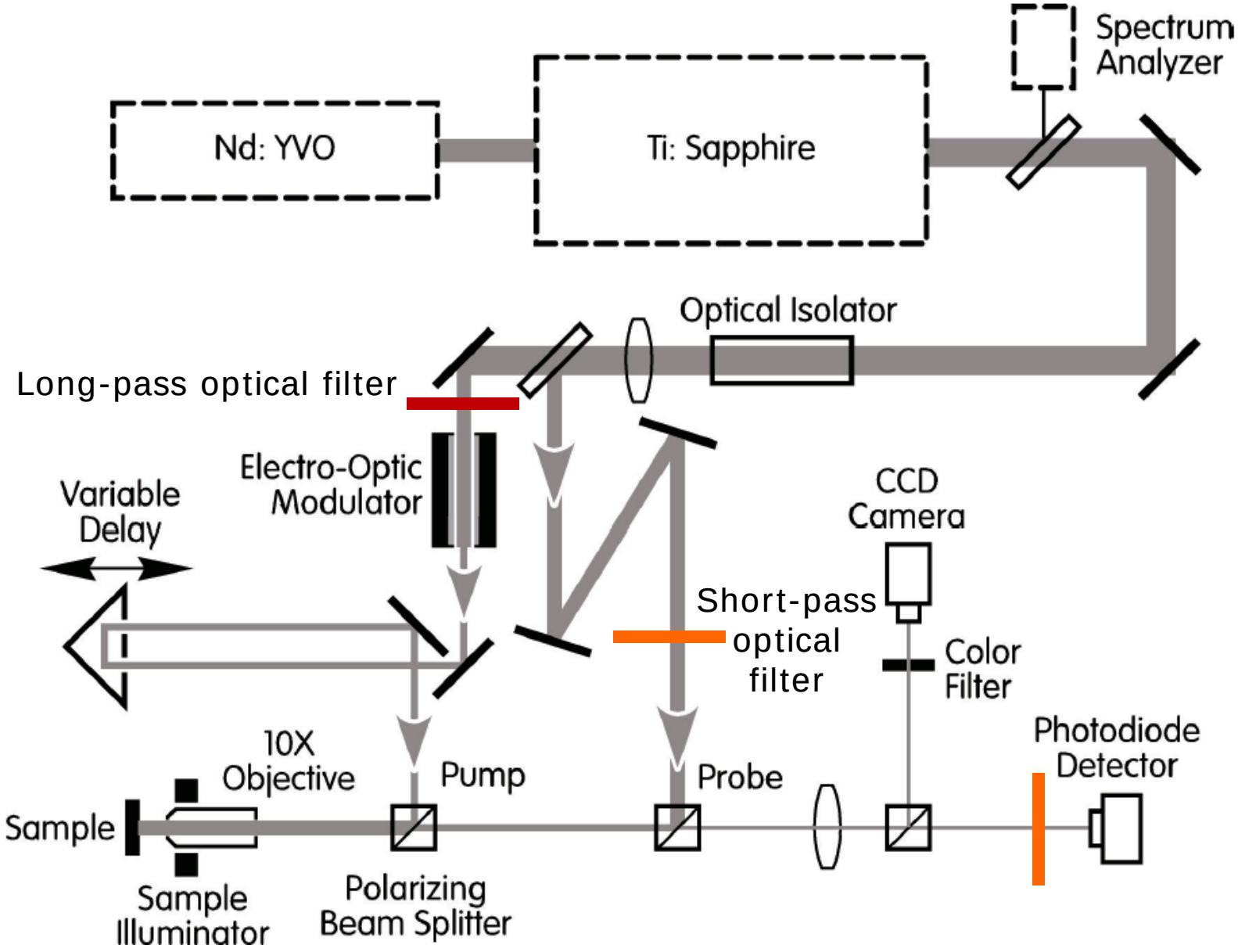

TDTR received the 2018 *Innovation in Materials Characterization Award* from the Materials Research Society

Google scholar citation count in March 2019

Analysis of heat flow in layered structures for time-domain thermoreflectance DG Cahill	918	2004

Dozens of similar instruments in use world-wide for studying thermal transport

Clone built at Fraunhofer Institute for Physical Measurement, Jan. 7-8 2008

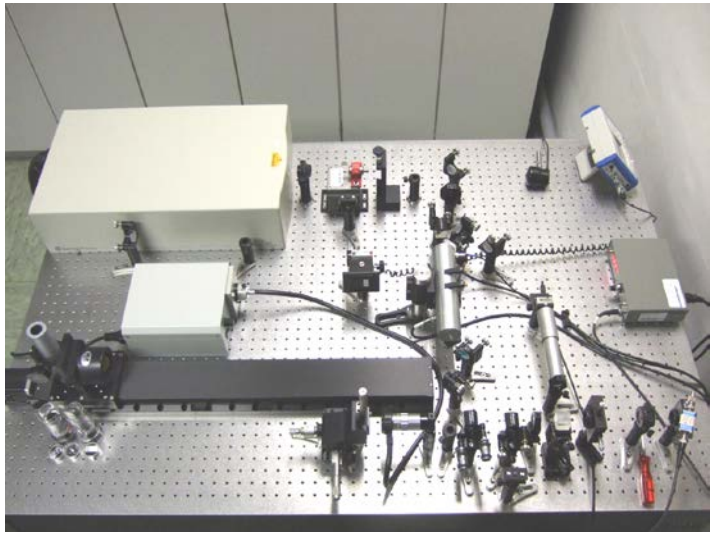

Excellent tutorial by Ronggui Yang's group at U. Colorado, *JAP* (2018)

psec acoustics and time-domain thermoreflectance

- Optical constants and reflectivity depend on strain and temperature
- Strain echoes give acoustic properties or film thickness
- Thermoreflectance dR/dT gives thermal properties

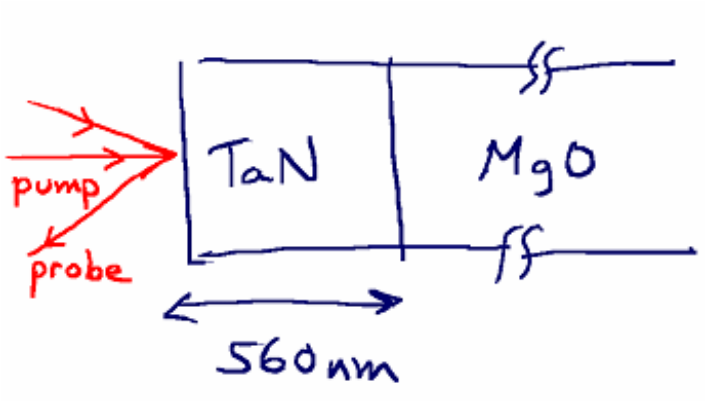

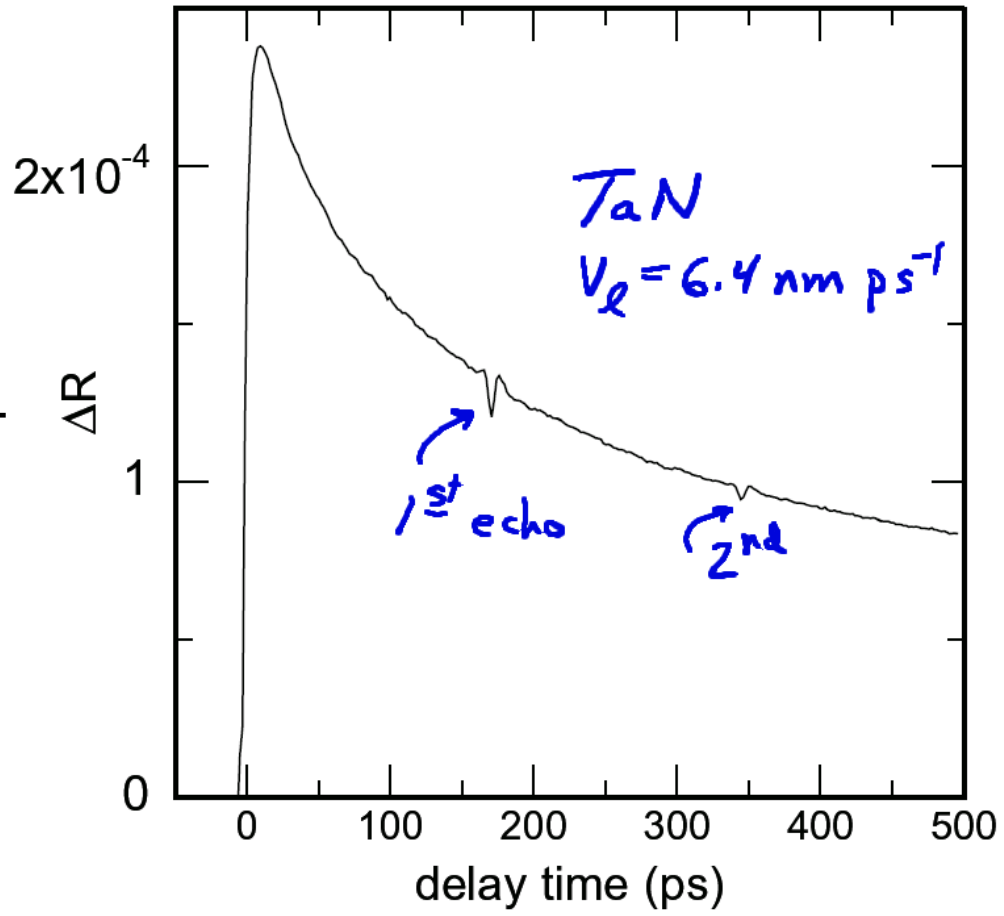

Large dR/dT is desired for higher signal-to-noise

R=optical reflectivity; T=temperature

Ti:sapphire laser

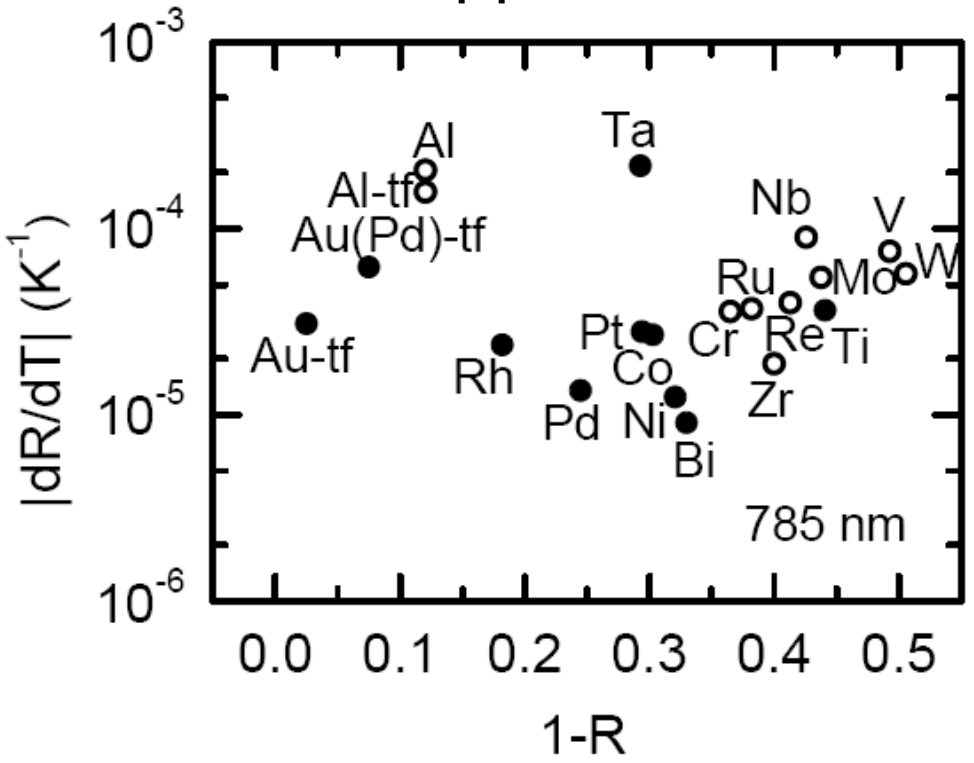

Wang *et al*., JAP (2010)

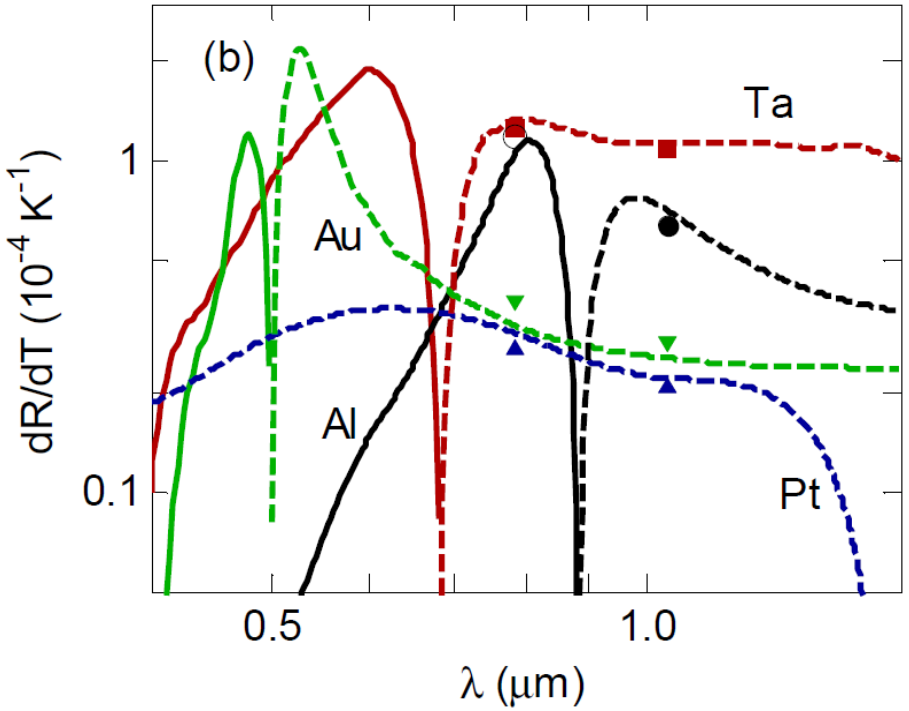

Wilson *et al*., Optics Express (2012)

Partial differential equations are difficult to solve so transform into an algebraic frequency domain equation in both time and space

- Diffusion equation is a linear equation as long as the temperature excursion are not too large as to create significant changes in Λ, C, or G.
  - Frequency/spatial-frequency domain solutions contain the same information as time/space solutions.

$$C\frac{dT}{dt} = \Lambda\nabla^2 T \quad \rightarrow \quad \tilde{T} = \tilde{T}_0 \exp(i\omega t)\exp(-qz)$$

$$i\omega C\tilde{T} = \Lambda q^2 \tilde{T}$$

$$q = \sqrt{\frac{i\omega}{D}}$$

Analytical solution to 3D heat flow in an infinite half-space, Cahill, RSI (2004)

- Gaussian-weighted surface temperature measured by the probe

$$\Delta \mathcal{T} = 2\pi A \int_0^\infty G(k) \exp\left(-\pi^2 k^2 \left(w_0^2 + w_1^2\right)/2\right)\ k\ dk$$

- Note the exchange symmetry of the pump and probe radius, w_0 and w_1
- This result is general: the solution must be independent of exchanging the role of heat sources and temperature measurements.
- For any linear problem, the Green's function solution has this symmetry (ρ is a position vector)

$$g(\rho, t; \rho' t') = g(\rho', -t'; \rho, -t)$$

Note about anisotropy

- Thermal conductivity is the second-rank tensor that relates vector heat flux to a vector temperature gradient. Cubic crystals, glasses and randomly oriented polycrystalline materials are isotropic.
- Simple matter to deal with in-plane vs. through thickness anisotropy: Use in-plane thermal conductivity to calculate the D_n terms.
- Full tensor description is available. Need is rare but has come up recently in our studies of the transverse thermal conductivity of polymer fibers, magnon thermal conductivity of cuprates, thermal conductivity of orthorhombic 2D materials.

Frequency domain solution

- Comparison of Al (100 nm)/SiO2 (100 nm)/Si and Al/Si
- Solid lines are real part; dashed lines are imaginary part

Note the peak in the imaginary part for $Al/SiO_2/Si$ near 10 MHz.

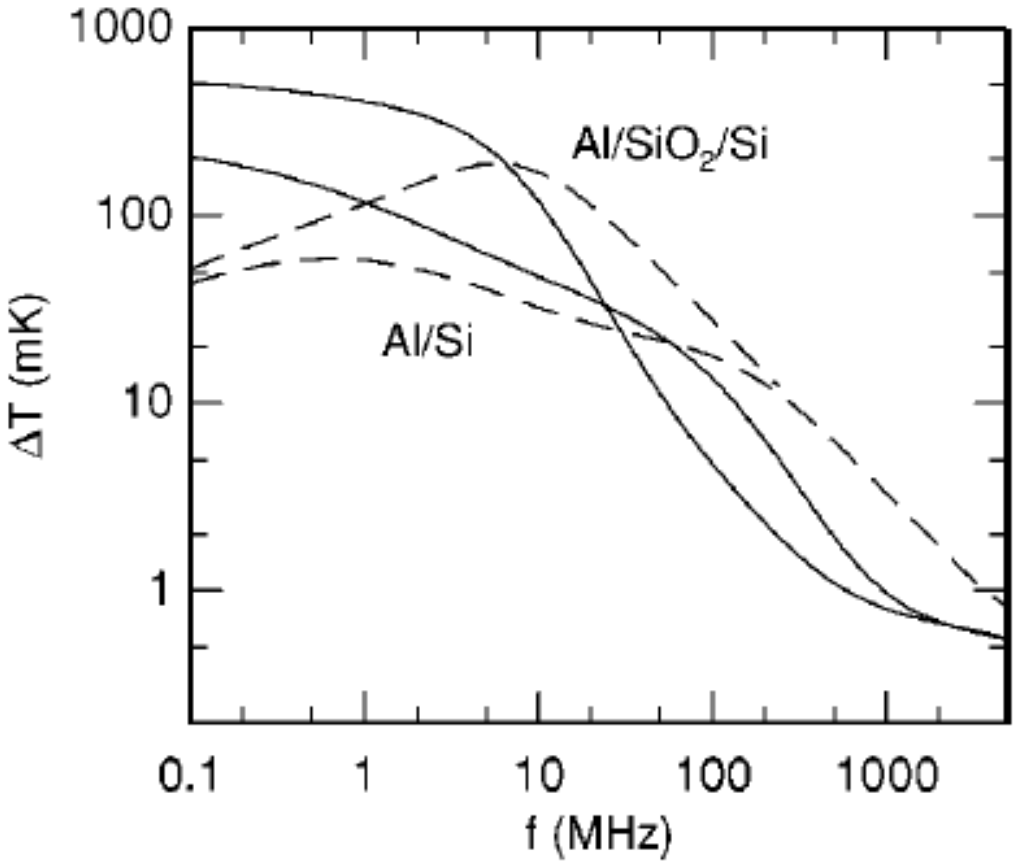

Signal analysis for the rf lock-in

- In-phase and out-of-phase signals by series of sum and difference over sidebands

$$\mathrm{Re}\left[\Delta R_M(t)\right] = \frac{dR}{dT}\sum_{m=-M}^{M}\left(\Delta\mathcal{T}(m/\tau+f)+\Delta\mathcal{T}(m/\tau-f)\right)\exp(i2\pi mt/\tau)$$

$$\mathrm{Im}\left[\Delta R_M(t)\right] = -i\frac{dR}{dT}\sum_{m=-M}^{M}\left(\Delta\mathcal{T}(m/\tau+f)-\Delta\mathcal{T}(m/\tau-f)\right)\exp(i2\pi mt/\tau)$$

- out-of-phase signal is dominated by the $m=0$ term (frequency response at modulation frequency f)
  - ➢ This term carries most of the information about the thermal conductivity of the sample.

View of pulse accumulation in the time domain

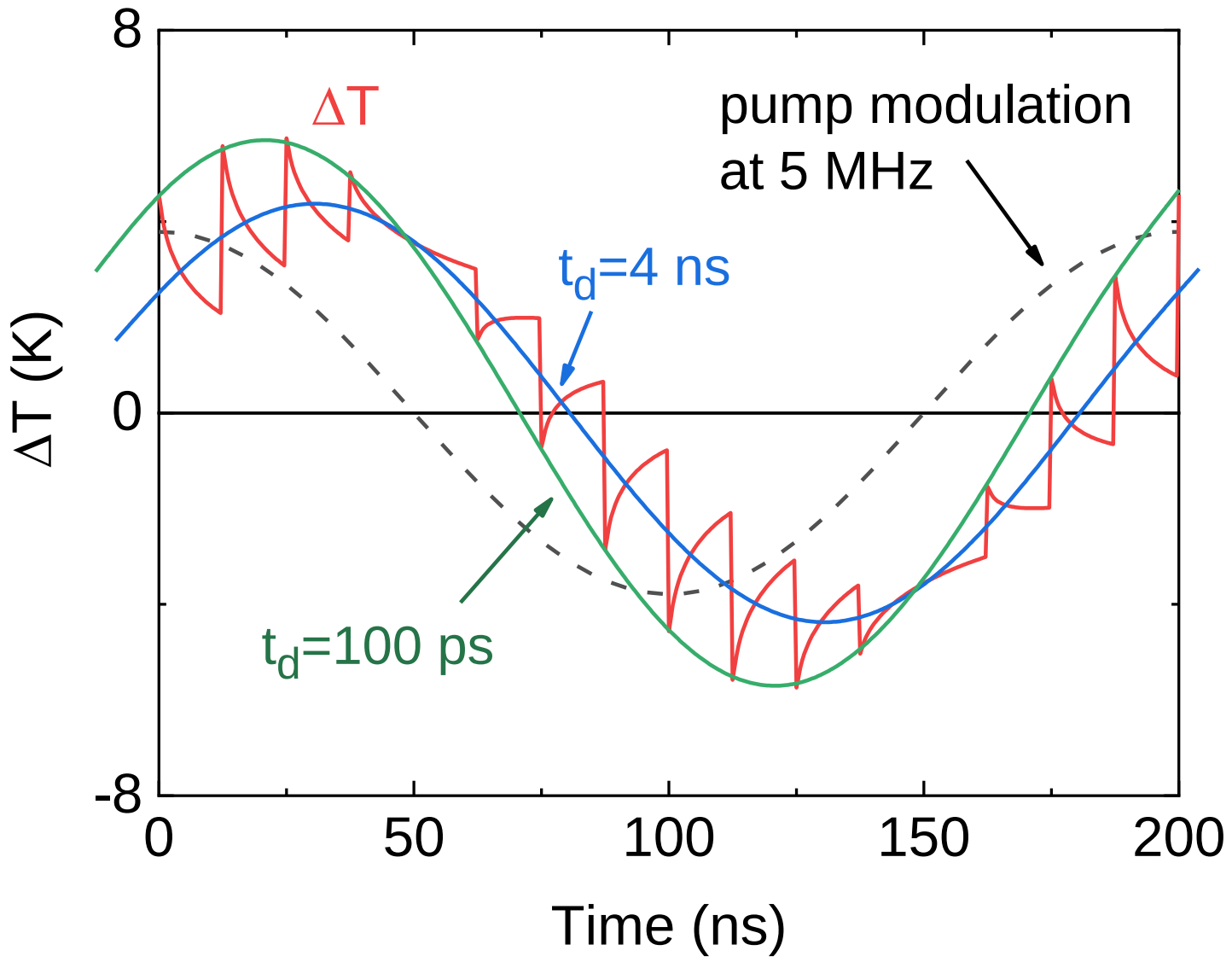

Time-domain Thermoreflectance (TDTR) data for $TiN/SiO_2/Si$

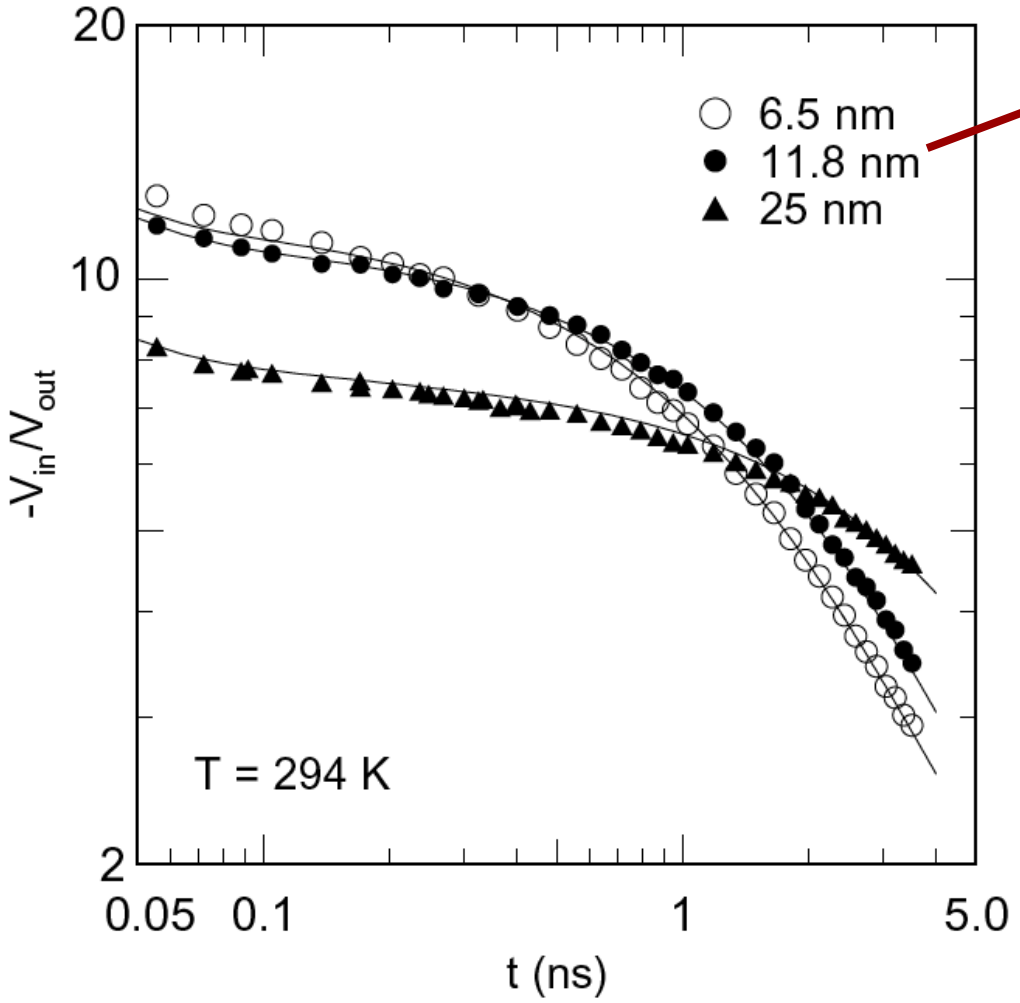

Costescu *et al*., PRB (2003)

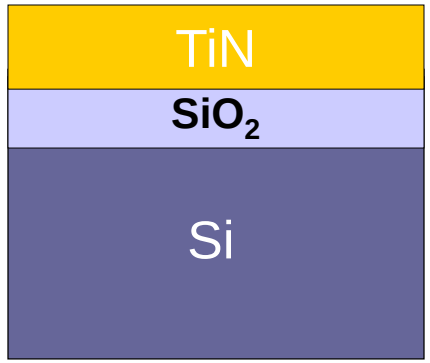

- reflectivity of a metal depends on temperature
- one free parameter: the “effective” thermal conductivity of the thermally grown SiO_2 layer (interfaces not modeled separately)

Validation experiments for thin films and bulk

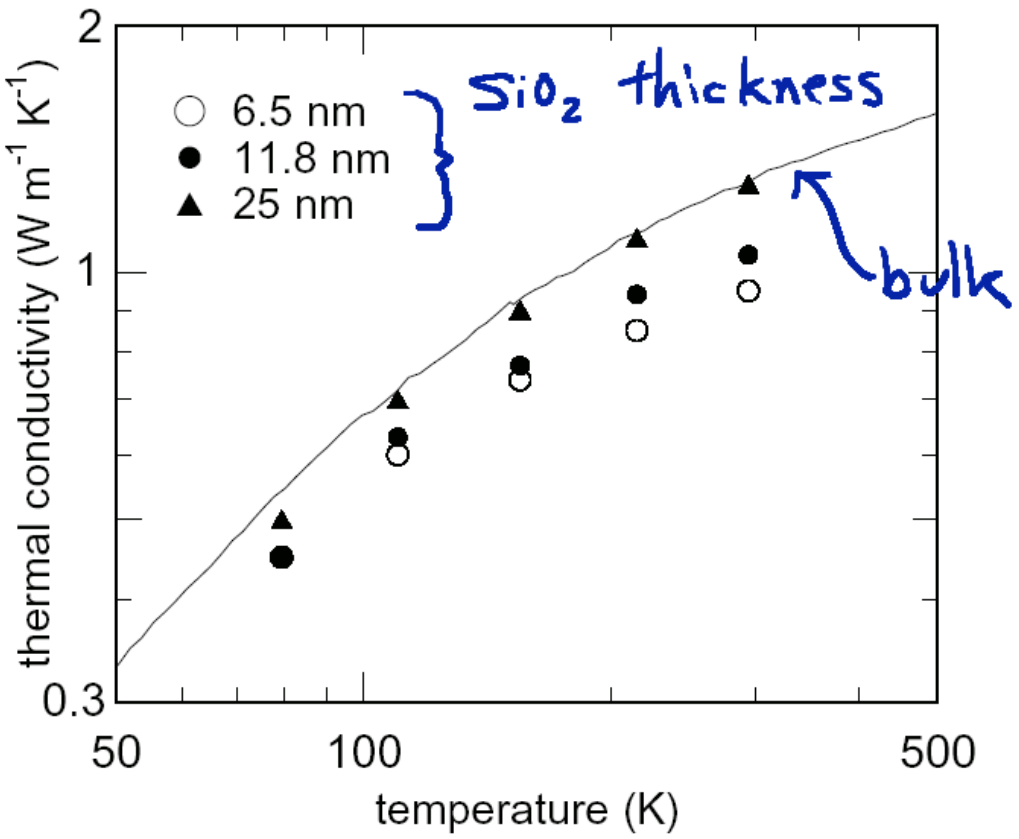

Costescu *et al*., PRB (2003)

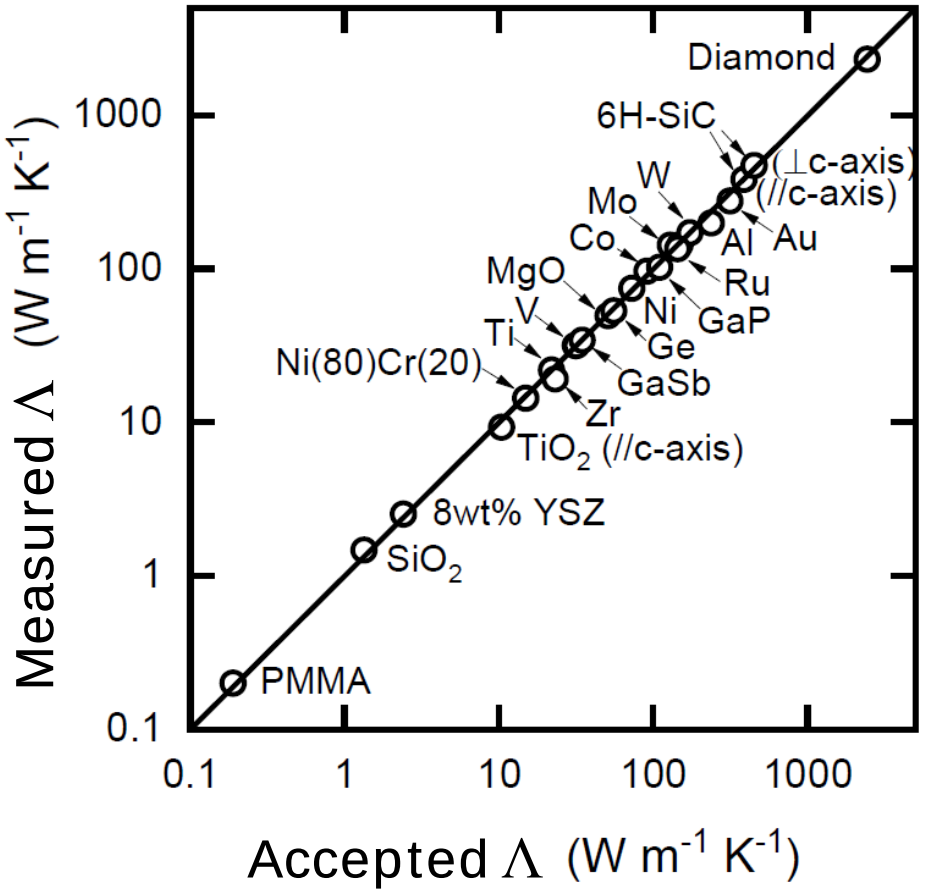

Jiang *et al*., JAP (2018)

Quantify the sensitivities using the logarithmic derivative of the ratio signal with respect to experimental parameters

- Example of sensitivity to the interface thermal conductance

$$\phi(t) = -\frac{V_{in}(t)}{V_{out}(t)}$$

$$S_G(t) = \frac{d\ln\left(\phi(t)\right)}{d\ln G}$$

- If for small changes in G, $\phi \propto G^{\beta}$ then $S_G = \beta$

Quantify the sensitivities using the logarithmic derivative of the ratio signal

- Example of sensitivity to the interface thermal conductance *G* and thermal conductivity (κ in this plot) at two delay times, 200 ps and 4 ns.

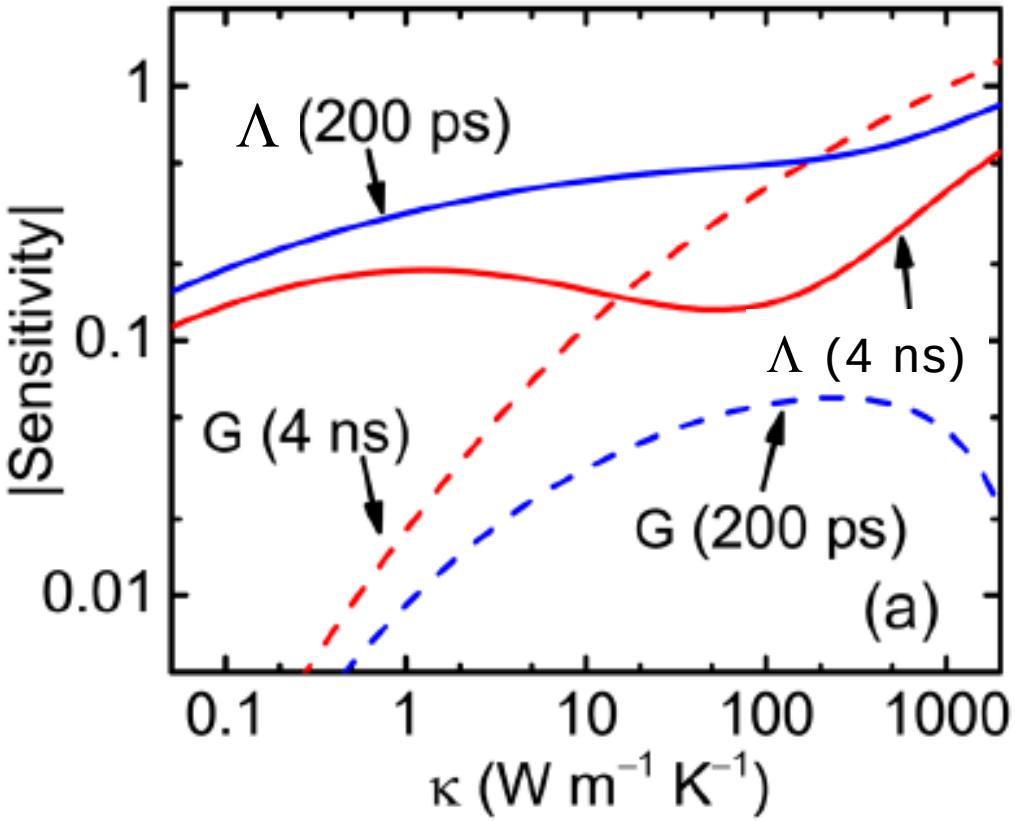

$w_0 = 10$ μm

$G = 200$ MW m^{-2} K^{-1}

Sensitivities are the key to analyzing uncertainties and error propagation

- For example, error propagation from an uncertainty in metal film thickness Δh to an uncertainty in thermal conductivity

$$\Delta\Lambda = \frac{S_h}{S_\Lambda}\Delta h$$

- Typical numbers,

$S_h \approx 1$; $S_\Lambda \approx 0.5$; $\Delta h = 5\%$ ➔ $\Delta\Lambda = 10\%$

Thickness of the transducer places a limit on our ability to see what happens in a material at short time scales

- Limited by interface conductance.
  - Equivalent to discharging of a capacitor through a resistor

$$\tau_G = \left(\frac{1}{AG}\right)(VC) = \frac{hC}{G}$$

h = 60 nm; C = 2.5 MJ m^{-3} K^{-1}; G = 200 MW m^{-2} K^{-1}

τ_G = 0.75 ns

What could we do if the transducer was 6 nm thick instead of 60 nm thick?

- Access time scales in high thermal conductivity crystals down to ~100 ps.
- Increase sensitivity to low thermal conductivity materials by reducing the product of modulation frequency (f = 10 MHz) and the cooling time of the transducer.
- Reduce parasitic in-plane thermal conductance of the metal film transducer, ultimately $h\Lambda_f$ ~0.1 μW K^{-1}
  - In our initial work using TR-MOKE,

    $h\Lambda_f$=0.4 μW K^{-1} (vs. 10 μW K^{-1} for Al in TDTR)

    1.5 μW K^{-1} for NbV in TDTDR

In TR-MOKE, dθ/dT replaces dR/dT of a conventional thermoreflectance measurement

Kerr rotation

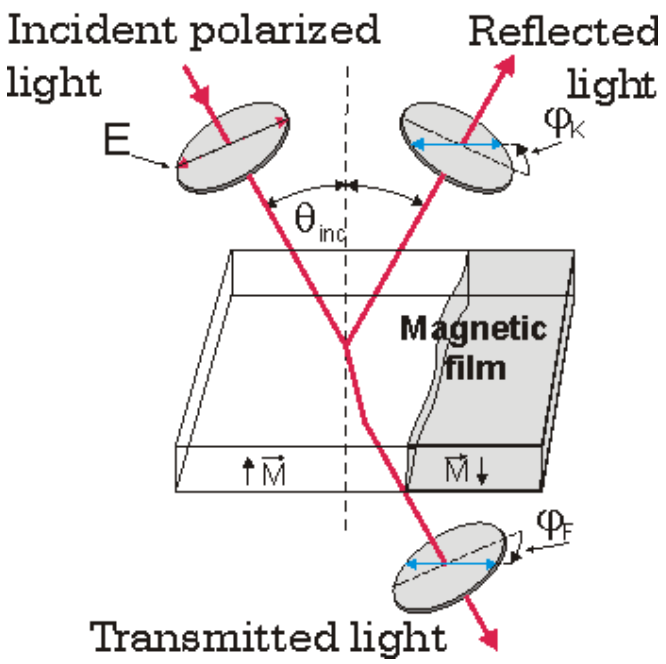

Faraday rotation

http://labfiz.uwb.edu.pl

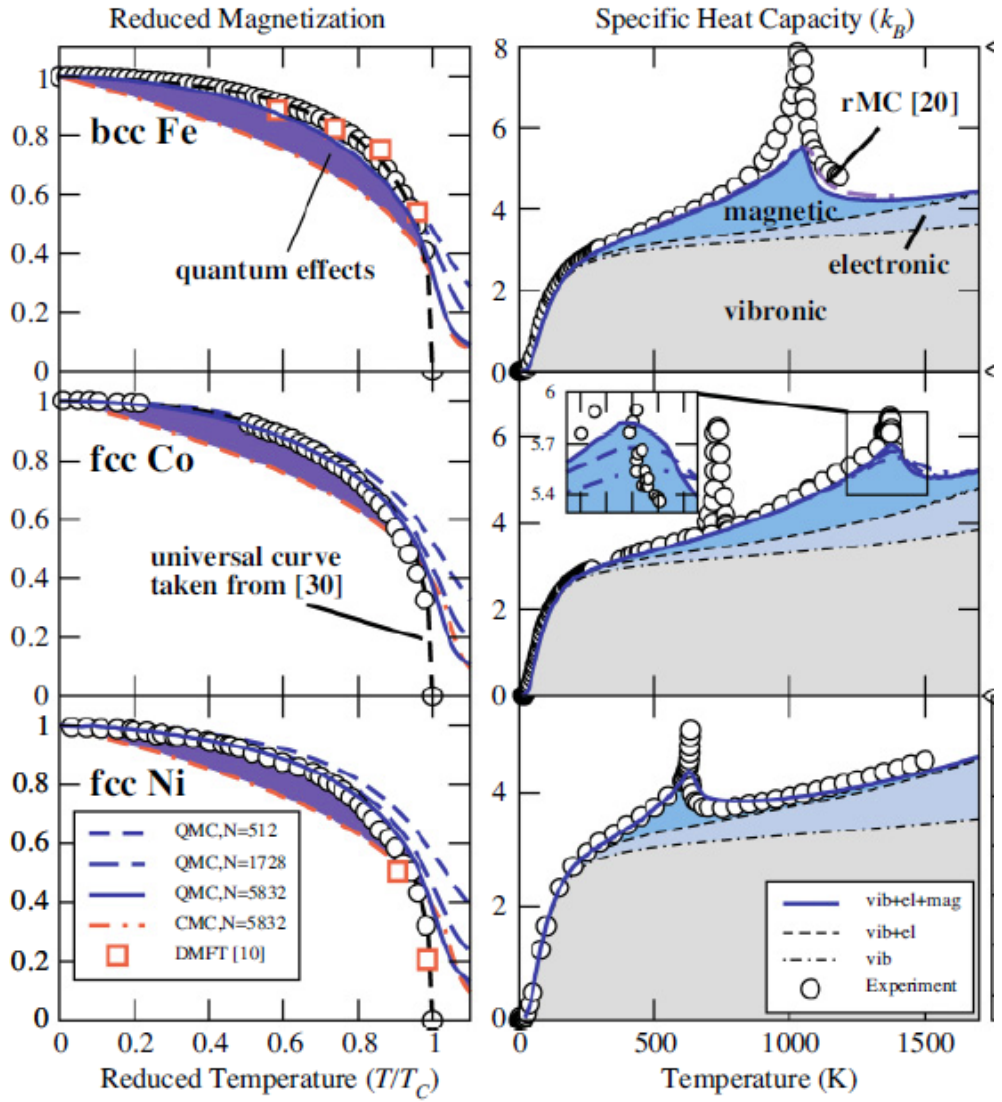

Körmann *et al*., PRB (2011)

Time-resolved magneto-optic Kerr effect (TR-MOKE)

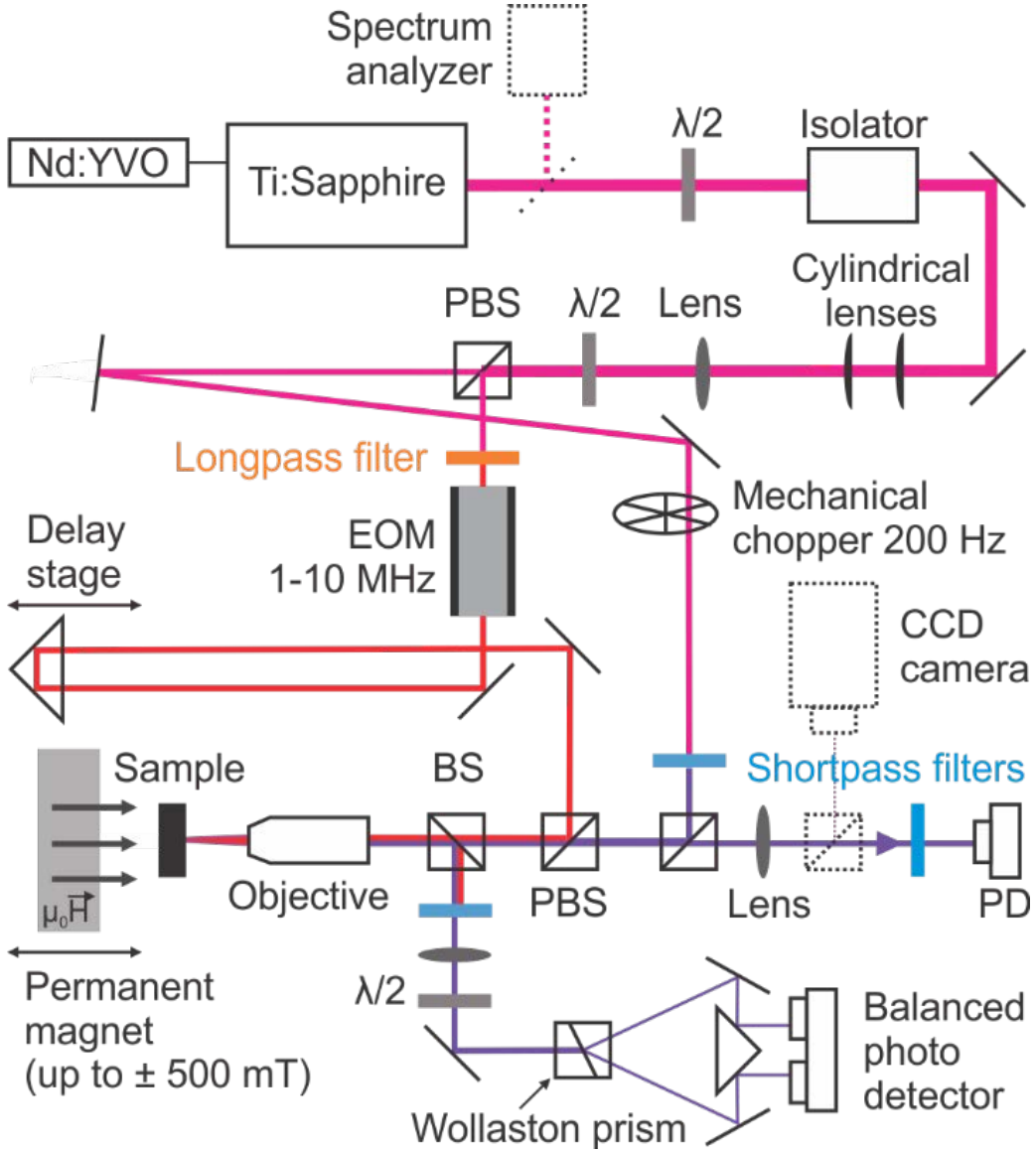

Kimling *et al.*, PRB (2017)

Perpendicular magnetic materials are the most convenient (polar Kerr effect)

- [Co,Pt] multilayers, 5-20 nm, sputter deposit at room temperature.

$$\frac{d\theta}{dT} \approx 10^{-5}\ \mathrm{K}^{-1}$$

- $L1_0$ phase FePt:Cu, 5 nm, sputter deposit at room temperature followed by rapid thermal annealing to 600 ºC.

$$\frac{d\theta}{dT} \approx 8\times10^{-5}\ \mathrm{K}^{-1}$$

- Amorphous TbFe (Xiaojia Wang at UMN), 25 nm, sputter deposit, cap with Ta.

$$\frac{d\theta}{dT} \approx 3\times10^{-5}\ \mathrm{K}^{-1}$$

Kerr signal from a semitransparent magnetic layer is only weakly dependent on dn_s/dT of the sample

- For an optically thin magnetic transducer of thickness *d*, index *n*, and magneto-optic coefficient *Q*, on a sample of index n_s.

$$\theta = \frac{Qn^2}{\frac{\lambda}{4\pi d}\left(n_s^2 - 1\right) + i\left(n_s^2 - n^2\right)}$$

- The critical parameter entering into $\frac{d\theta}{dT}$ is

$$\left|\frac{1}{Q}\frac{dQ}{dT}\right| \sim 10^{-2}\ \mathrm{K}^{-1} \quad \text{for [Co,Pt]}$$

Kerr signal from a semitransparent magnetic layer is only weakly dependent on dn_s/dT of the sample

- Worst case scenario where laser excitation of the Si substrate creates a strong contribution to the TDTR signal. By contrast, TR-MOKE is immune.

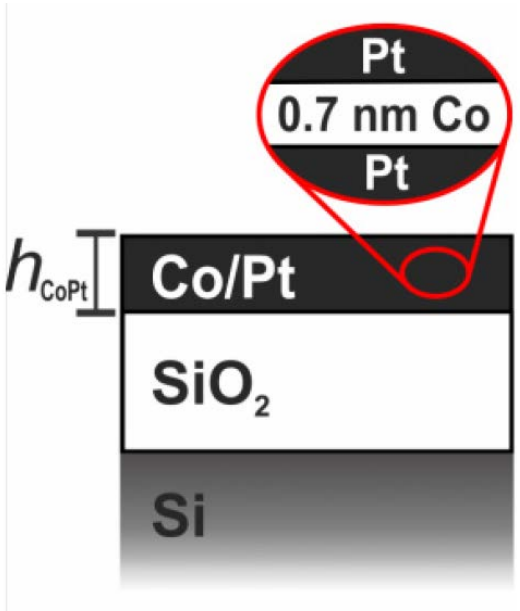

[Co,Pt](8 nm)/SiO_2(240 nm)/Si

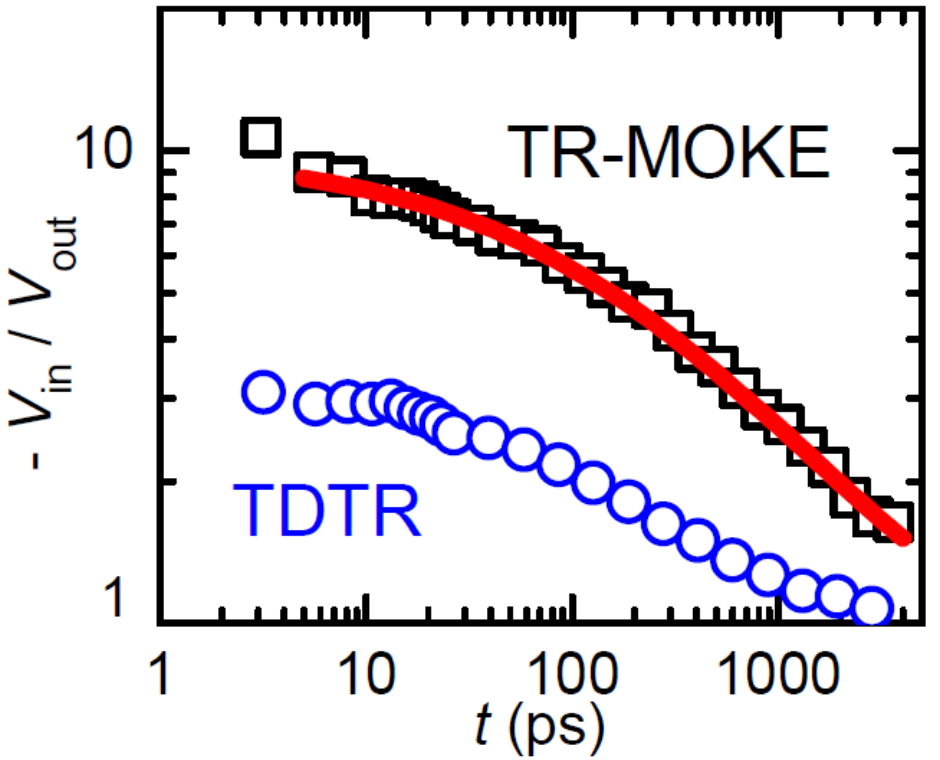

Kimling *et al*., PRB (2017)

Application to the thermal conductance of Pt/a-SiO2 interface

- Conventional TDTR lacks sufficient sensitivity because the Kaptiza length is much smaller than the metal film thickness.

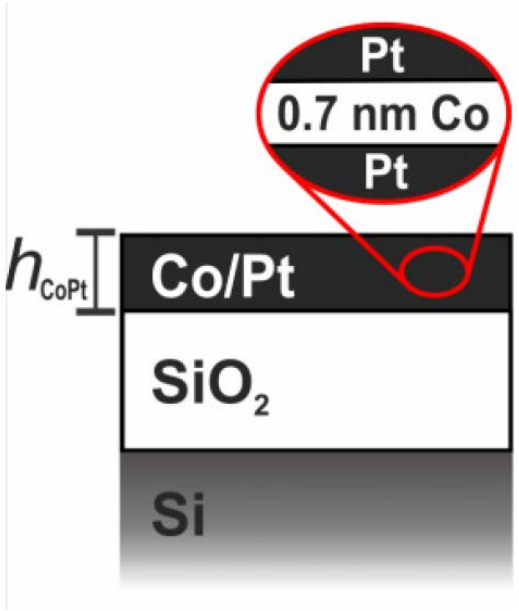

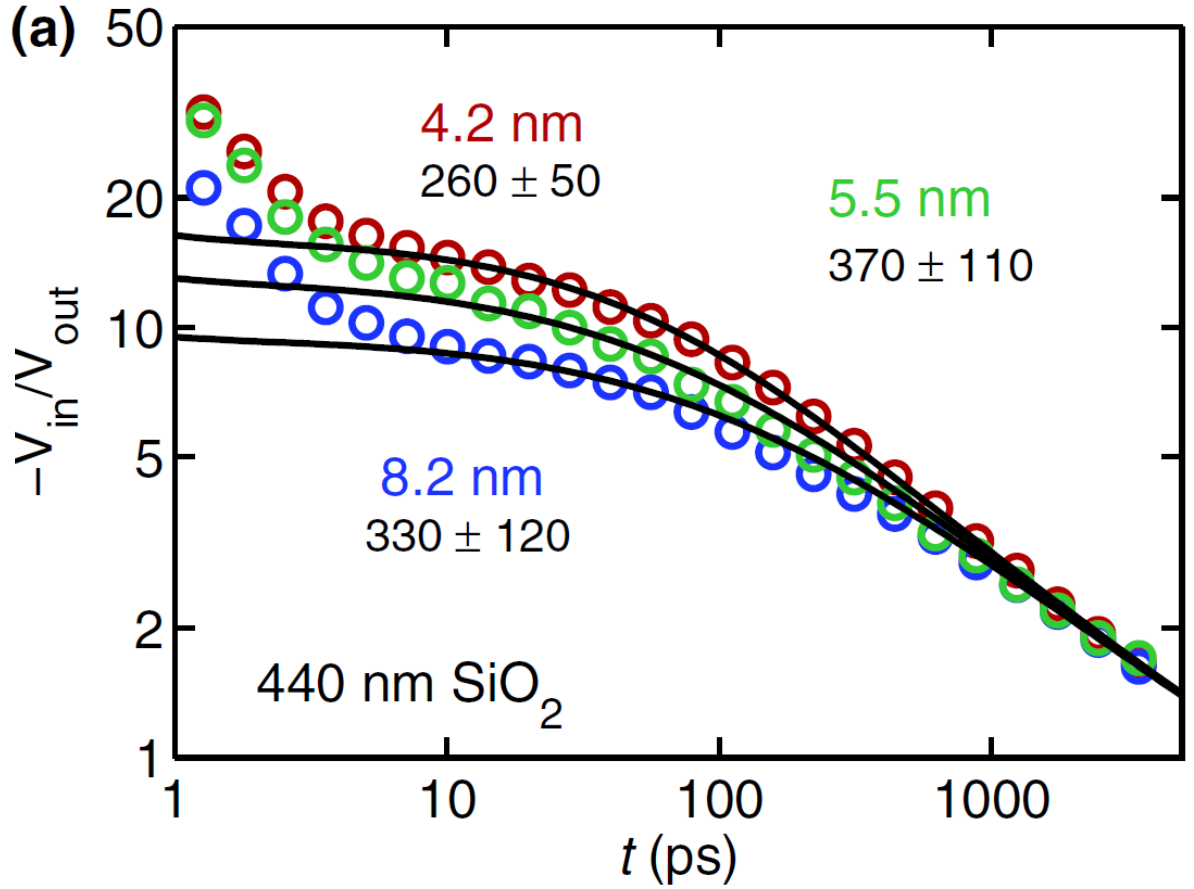

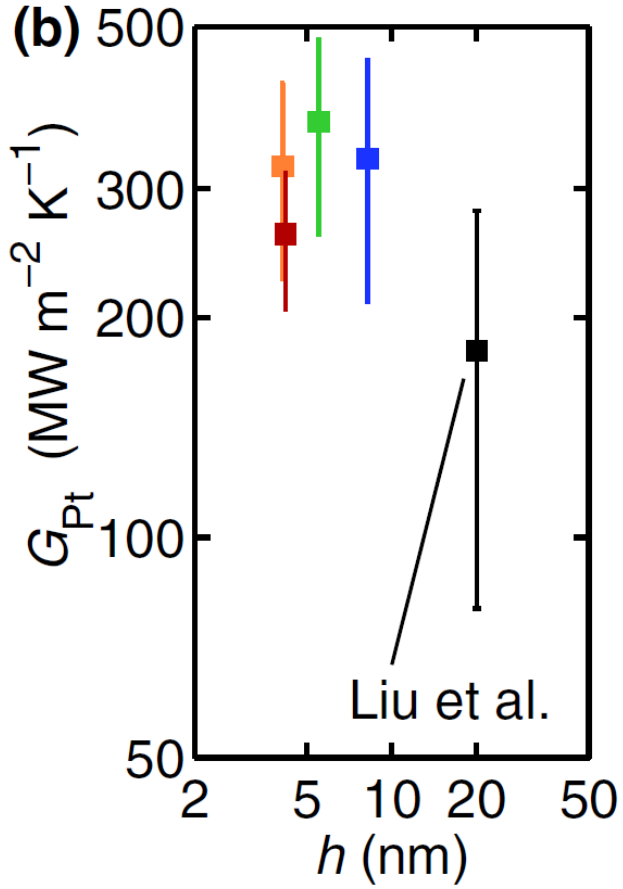

Kimling *et al.*, PRB (2017)

Take a critical look at the time resolution of a magnetic layer as a thermometer and its use as a thermometer for electronic temperature

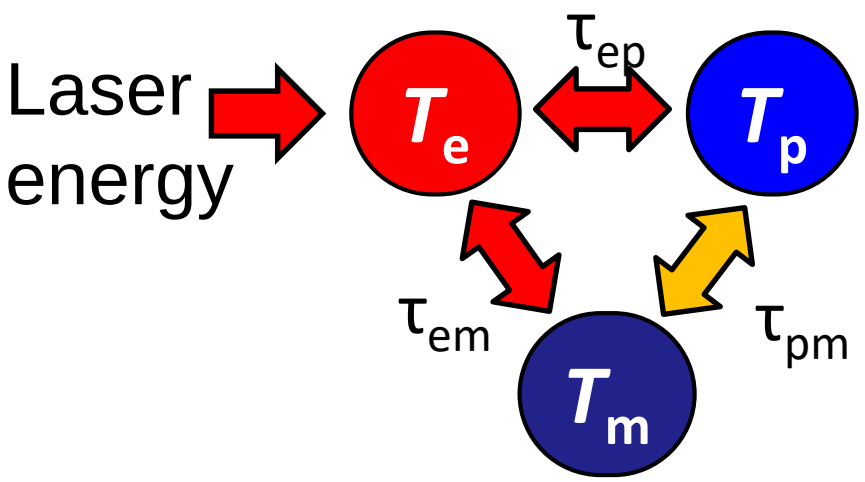

$$C_e(T_e)\frac{\partial T_e}{\partial t} = \frac{\partial}{\partial z}\left(\Lambda_e(T_e)\frac{\partial T_e}{\partial z}\right) - g_{ep}(T_e - T_{ph}) - g_{em}(T_e - T_m) + S(z,t)$$

$$C_{ph}\frac{\partial T_{ph}}{\partial t} = \Lambda_{ph}\frac{\partial^2 T_{ph}}{\partial z^2} + g_{ep}(T_e - T_{ph})$$

$$\tau_{em} = \frac{C_m}{g_{em}}$$

$$C_m\frac{\partial T_m}{\partial t} = \Lambda_m\frac{\partial^2 T_m}{\partial z^2} + g_{em}(T_e - T_m)$$

TR-MOKE of thin (0.8 nm) Co embedded near the middle of 6 nm of Pt

Pt(2)/**Co**(0.8)/Pt(4)/sapphire

Magnetic temperature (MOKE signal) is fit with two free parameters: electron-phonon coupling parameter of Pt and the relaxation time for Co magnons interacting with Co electrons

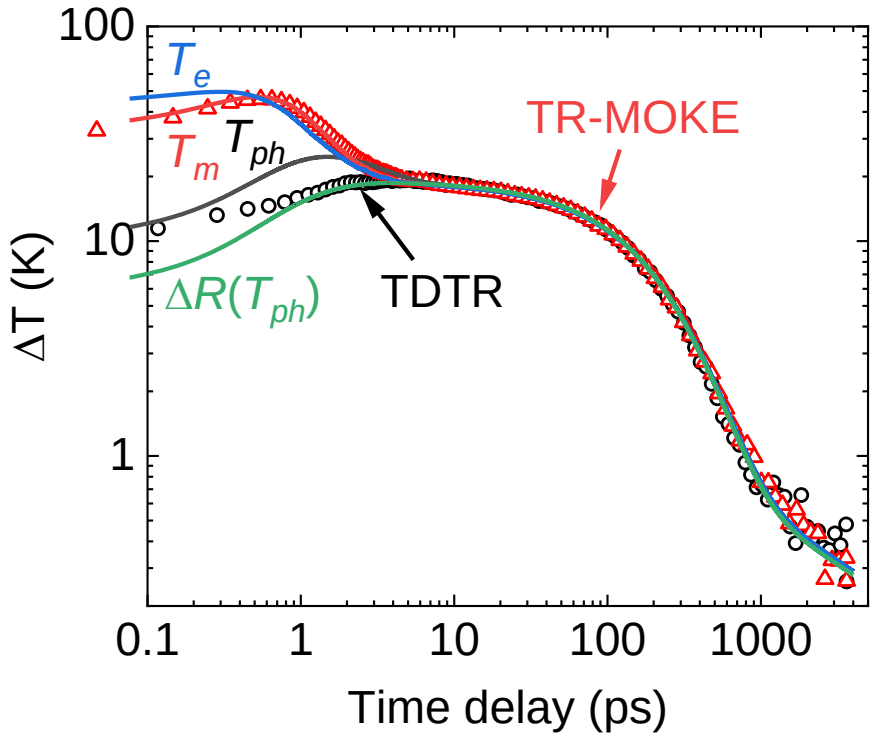

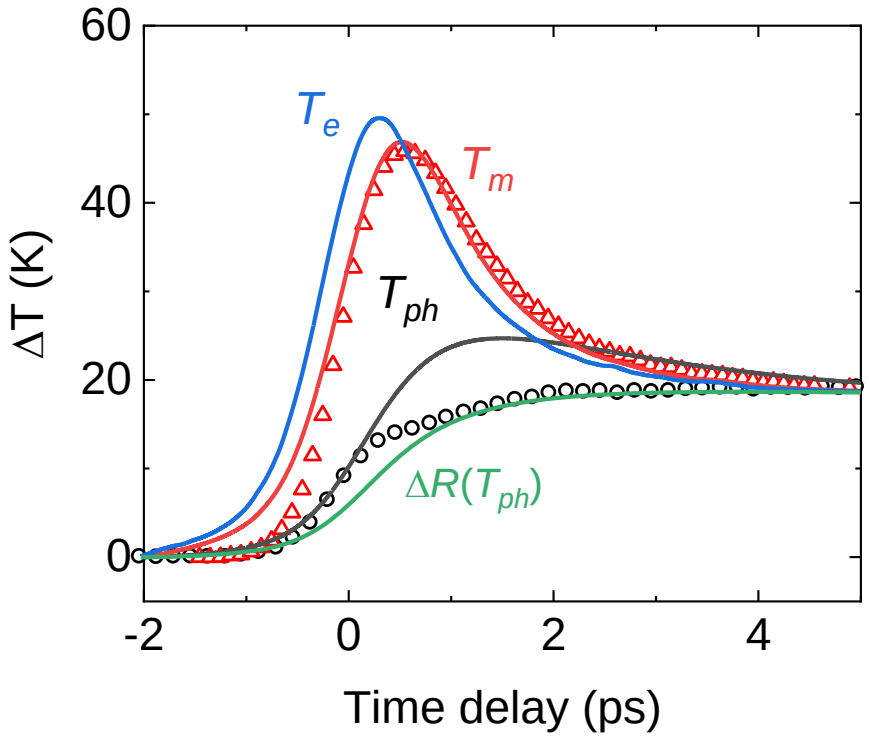

Jang, submitted

An electronic thermal transport version of “flash diffusivity” measurement

Pt(42)/**Co**(0.6)/Pt(4.2)/sapphire

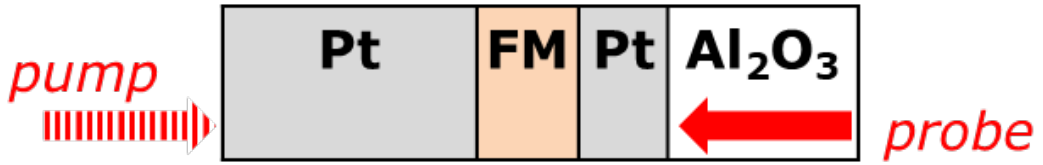

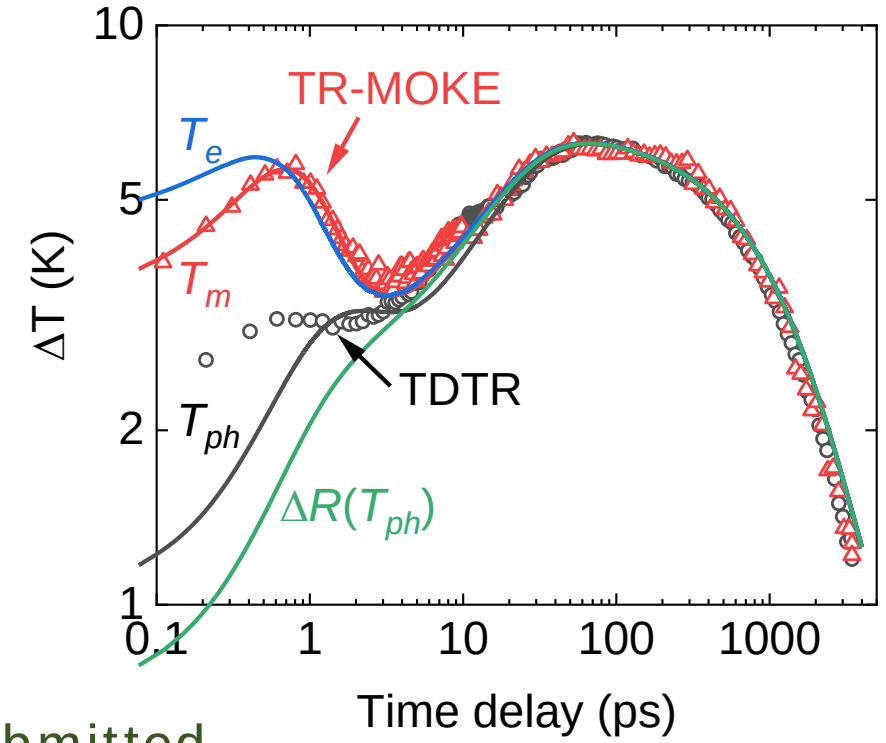

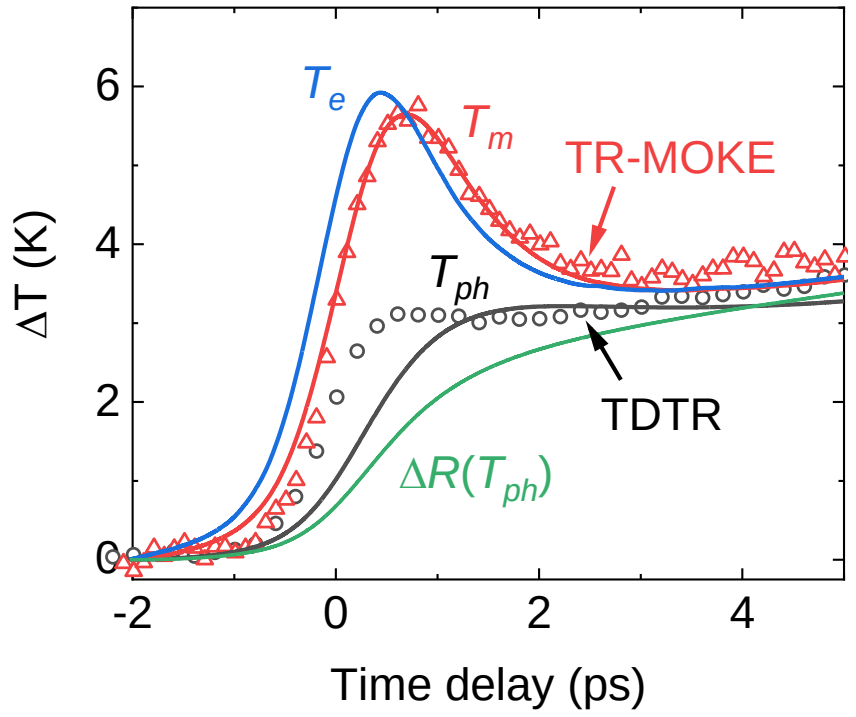

Jang, submitted

Consistent parameters extracted from the three-temperature model

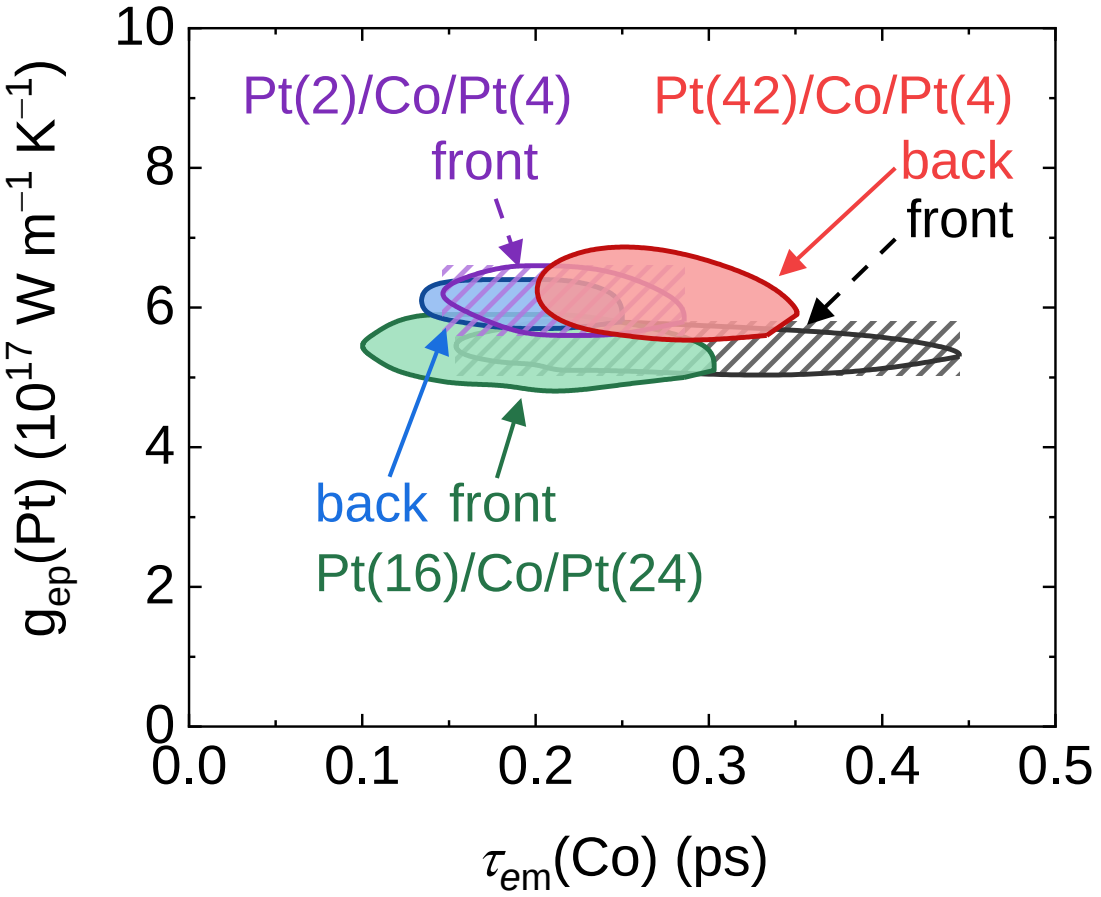

Jang, submitted

We are also interested in anti-ferromagnetic materials so explore terms in dielectric response that are quadratic in magnetization

$$\varepsilon_{ij} = \varepsilon_{ij}^{(0)} + \left[\frac{\partial \varepsilon_{ij}}{\partial M_k}\right]_{\mathbf{M}=0} M_k + \frac{1}{2}\left[\frac{\partial^2 \varepsilon_{ij}}{\partial M_k \partial M_l}\right]_{\mathbf{M}=0} M_k M_l + \ldots$$

$$= \varepsilon_{ij}^{(0)} + K_{ijk} M_k + G_{ijkl} M_k M_l + \ldots$$

Jana Hamrlová*, Jaroslav Hamrle, Kamil Postava, and Jaromír Pištora
Phys. Status Solidi B **250**, No. 10, 2194–2205 (2013)

magneto-optic Kerr
(anomalous) Hall
x-ray circular dichroism

quadratic magneto-optic Kerr
anisotropic magneto-resistance
x-ray linear dichroism

10 nm of Co has in-plane magnetization. Use data for two polarizations of the probe to separate the polar MOKE and magnetic birefringence

Polar MOKE measures out-of-plane magnetization

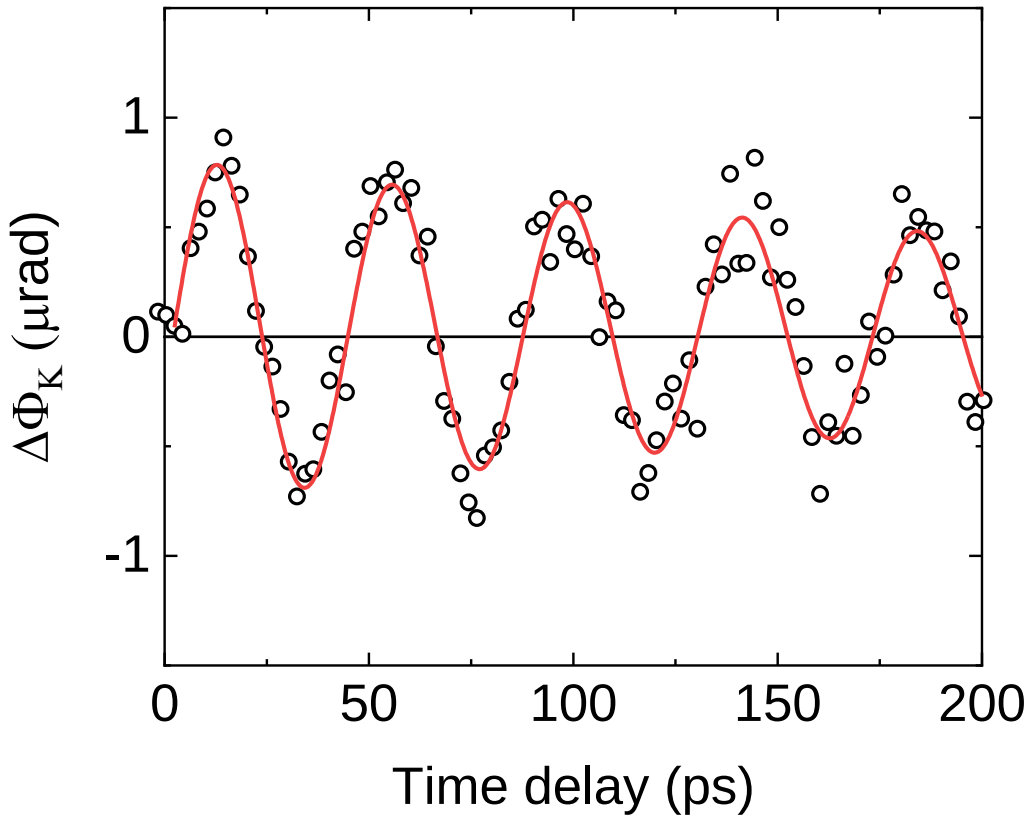

Magnetic birefringence measures changes in the square of the in-plane magnetization

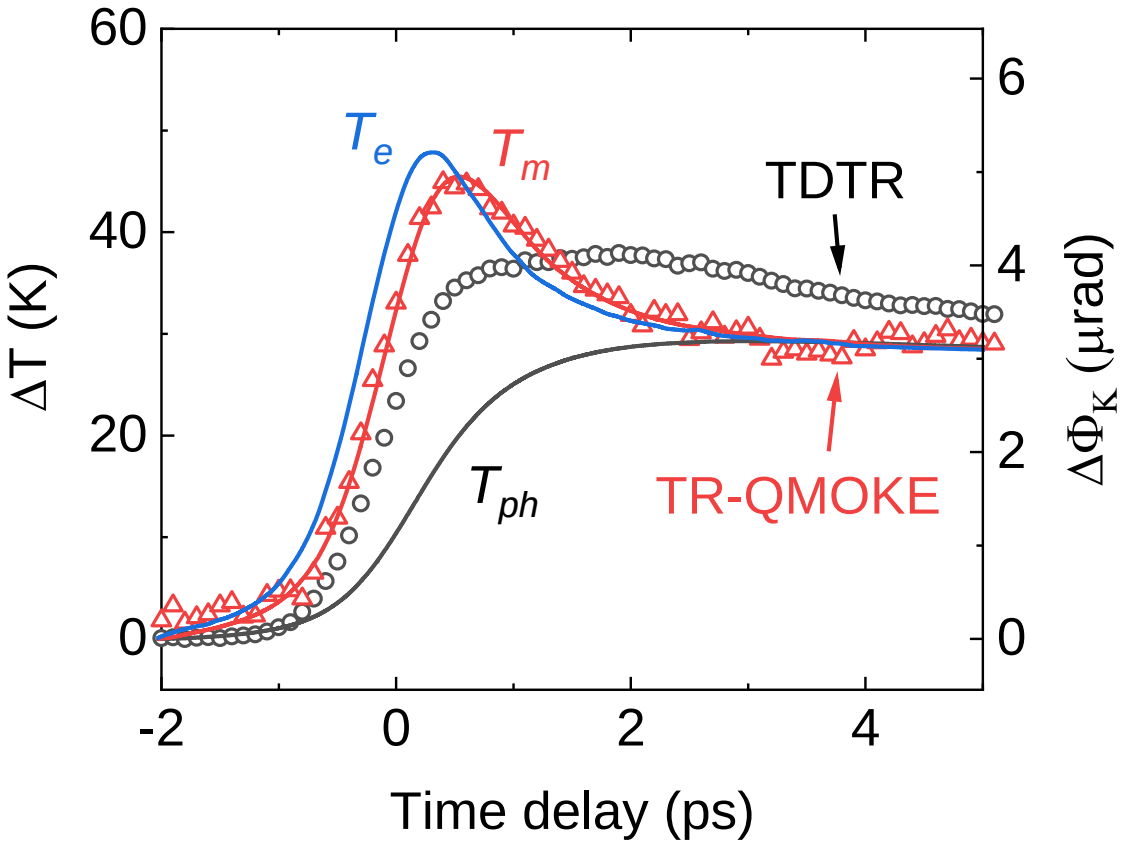

Jang, submitted

Magnetic birefringence can also be applied to anti-ferromagnets, materials with two opposing sub-lattice magnetization

Sweeping generalization: most ferromagnets are metals; most antiferromagnets are insulators

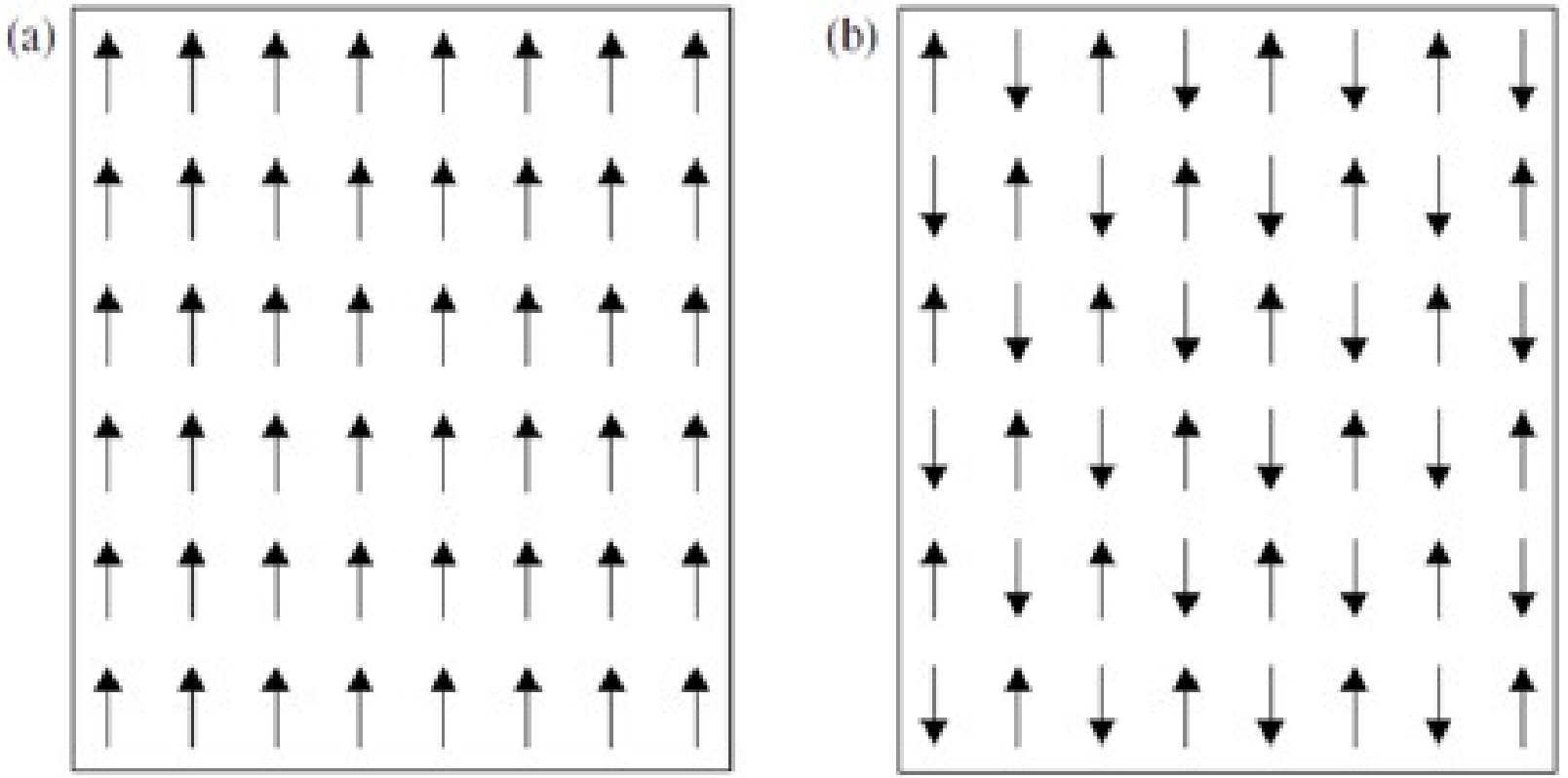

http://www.assignmentpoint.com/science/physics/antiferromagnetism-in-physics.html

insulating ferromagnet

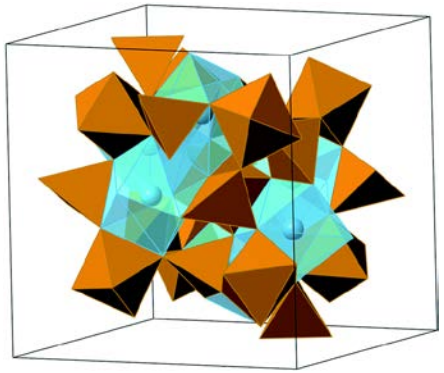

$Y_3Fe_5O_{12}$

Navrotsky et al., J Mat.Chem A (2014)

insulating antiferromagnet

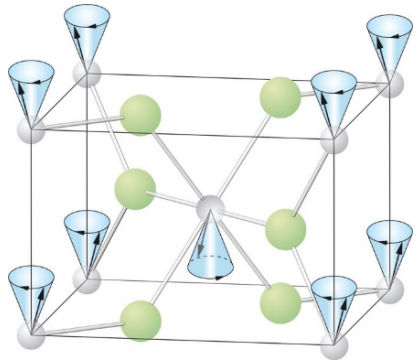

MnF_2

MPI for Solid State Physics

metallic ferromagnet

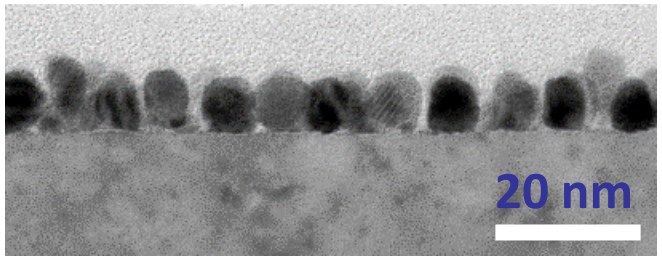

FePt:C granular media for heat-assisted recording

TEM by Hono group, NIMS

metallic antiferromagnet

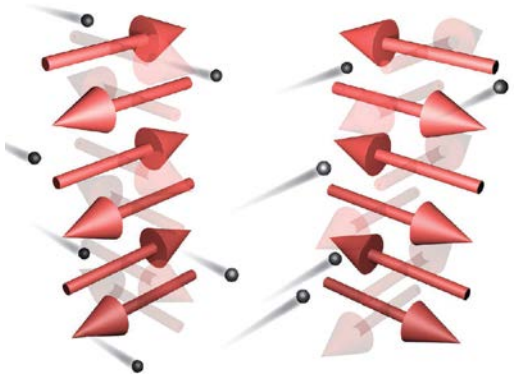

CuMnAs; Fe_2As;

MnPt; Mn_2Au

Fe_2As is a metallic antiferromagnet; tetragonal Cu_2Sb structure; T_N=350 K

The usual assumption is that the dominant quadratic magneto-optic term is longitudinal

$$\Delta\varepsilon_{11} = G_{11}M_1^{\ 2}$$

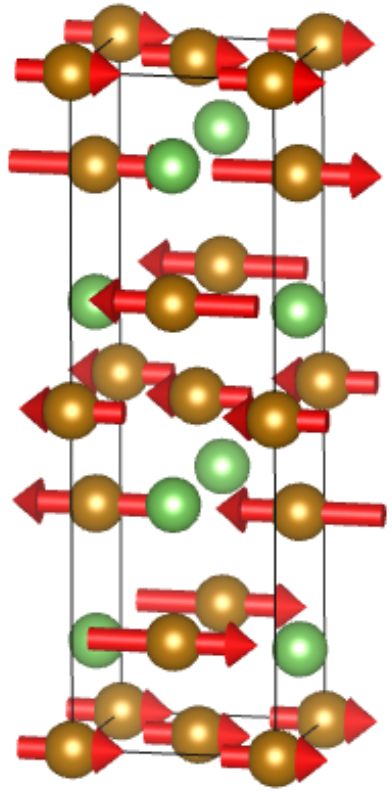

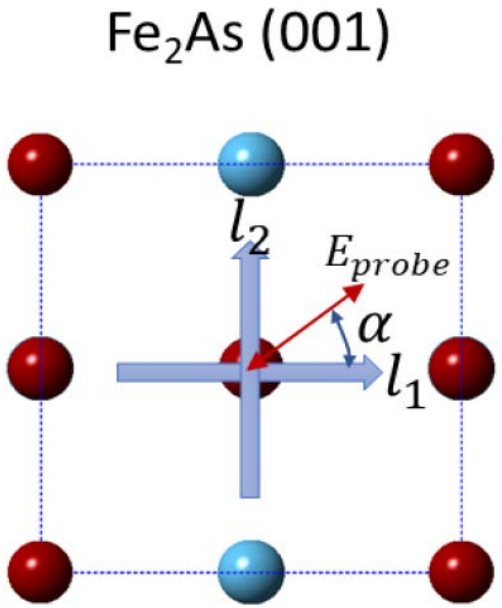

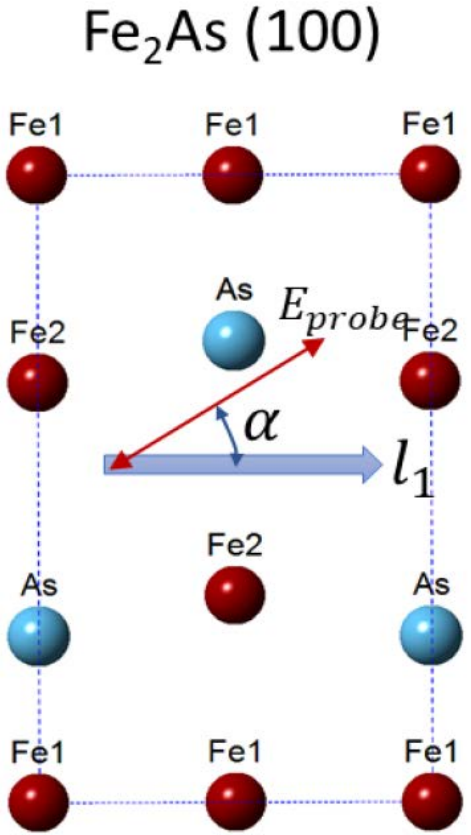

The longitudinal term, however, is weak. The dominant term is G_{31}

As expected for magnetic birefringence, the differential signal $d\theta/dT$ is proportional to the magnetic heat capacity

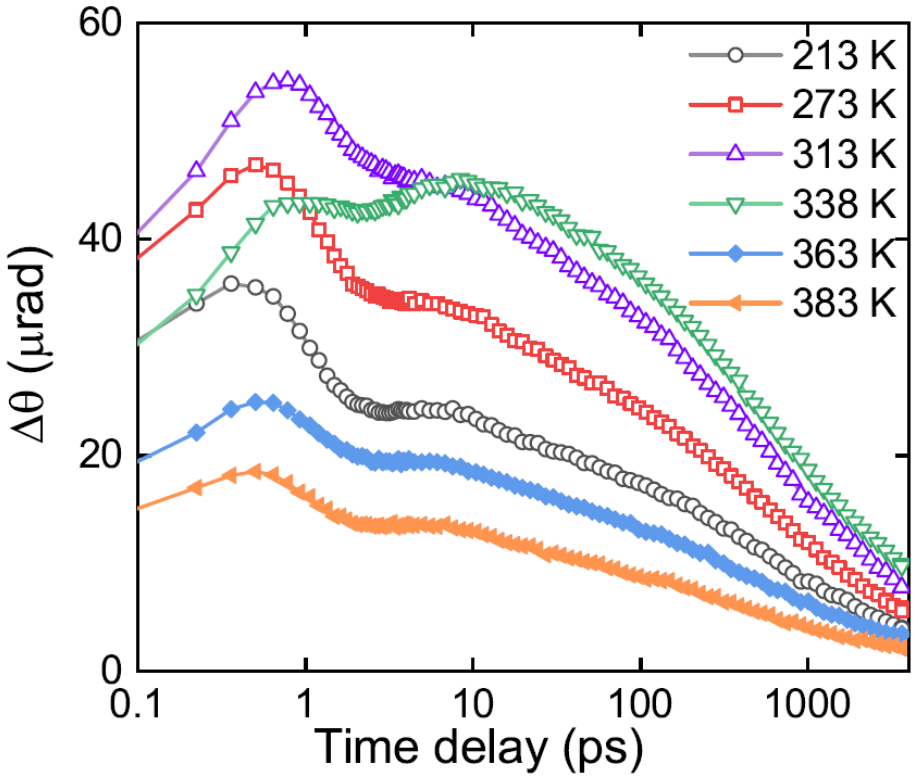

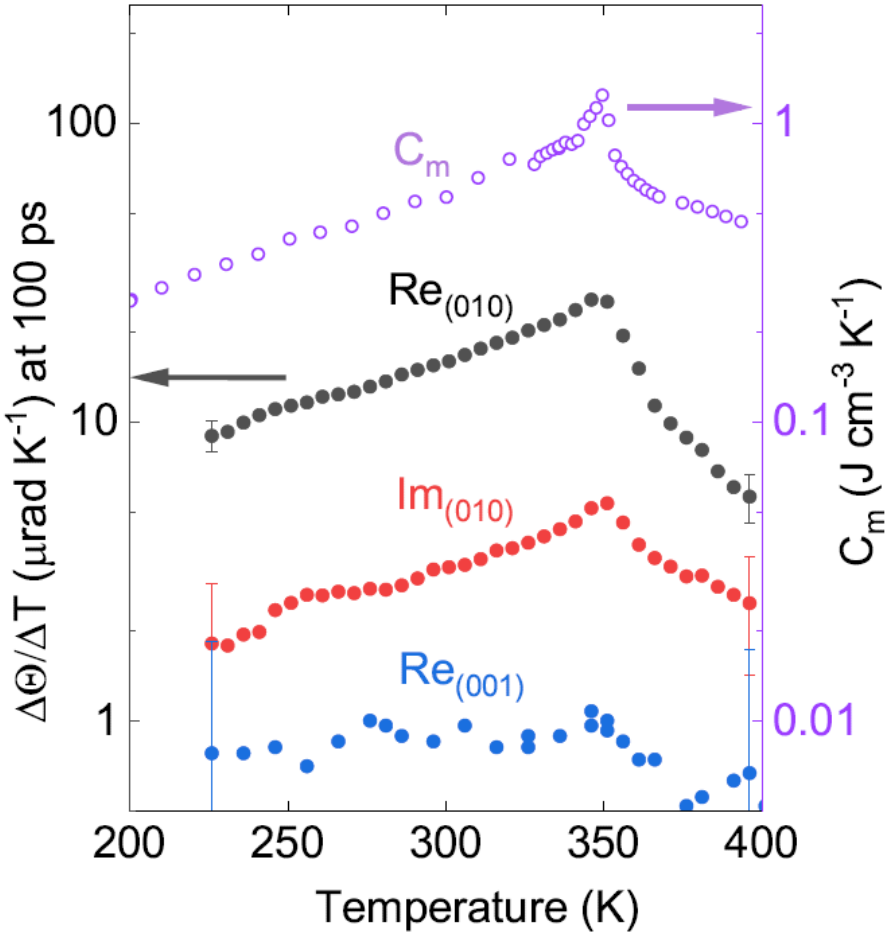

Yang, submitted

Thermal spin-transfer torque

Pt (20)/ [Co/Pt] or [Co/Ni] (3)/ Cu (100)/ CoFeB (2) (nm)

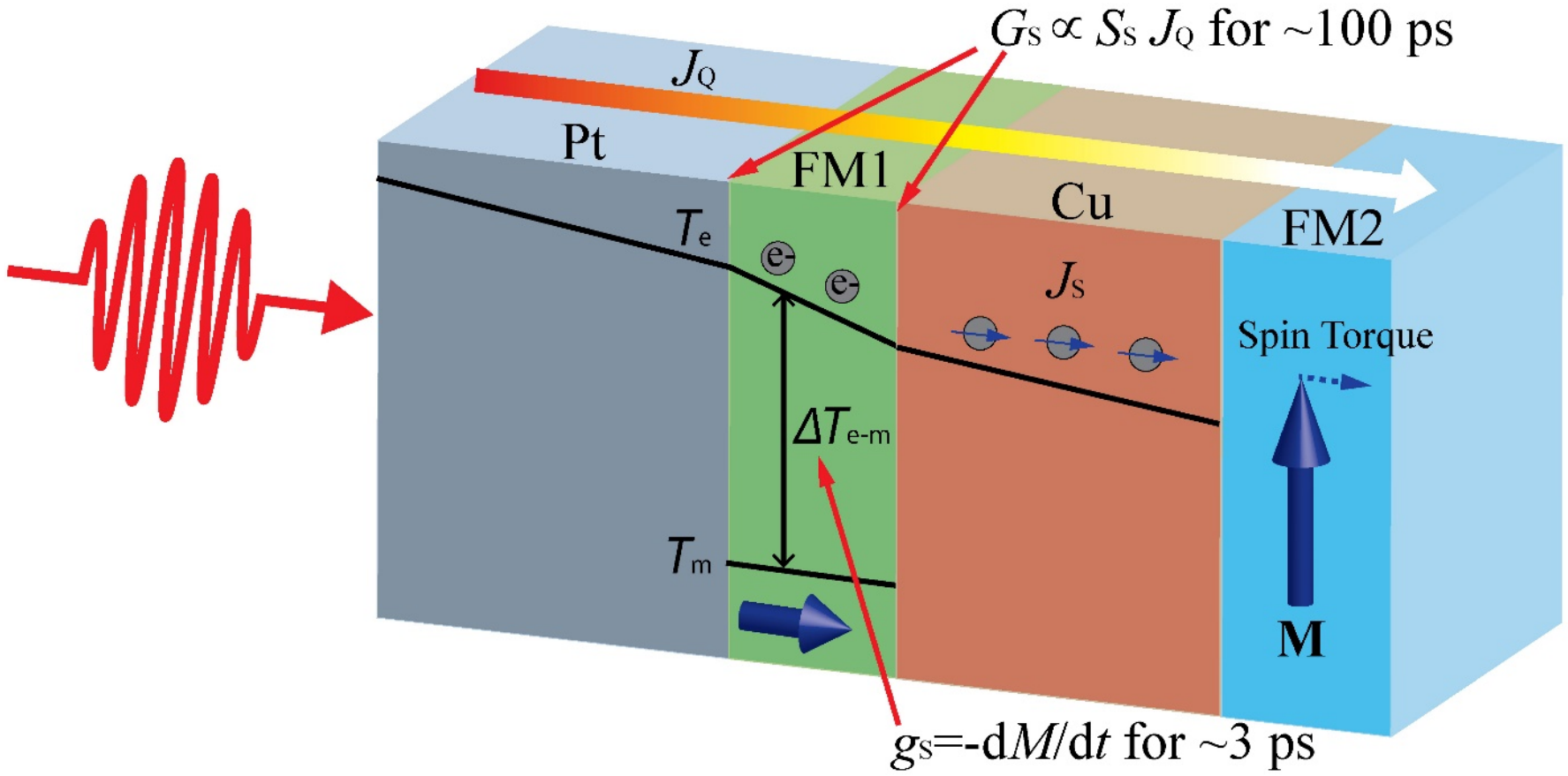

Choi, *et al.* Nature Physics (2015)

Two mechanisms for thermally-driven spin generation

Ultrafast demagnetization

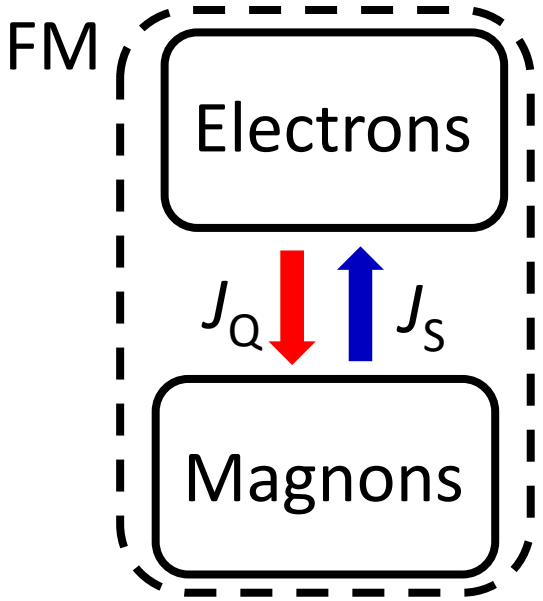

$$g_S = -\frac{dM}{dt}$$

Choi, *et al.* Nature Commun. **5**, 4334 (2014)

Spin-dependent Seebeck effect

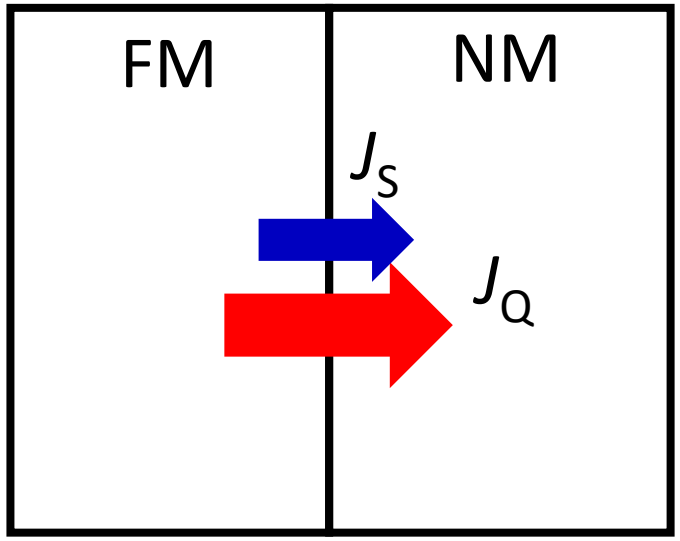

$$G_S = -\left(\frac{\mu_B}{eLT}\right) S_s J_Q$$

Slachter, *et al.* Nature Phys. **6**, 879 (2010)

Demagnetization-driven spin current (volume effect) during the time that magnons are out-of-equilibrium with electrons and phonons in the ferromagnet

Demagnetization

$$g_S = -\frac{dM}{dt}$$

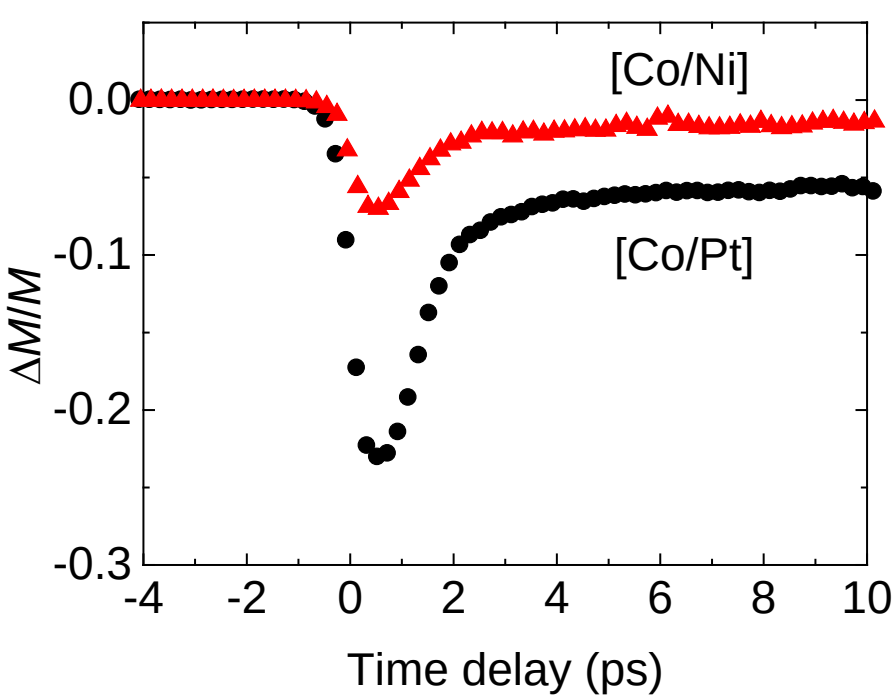

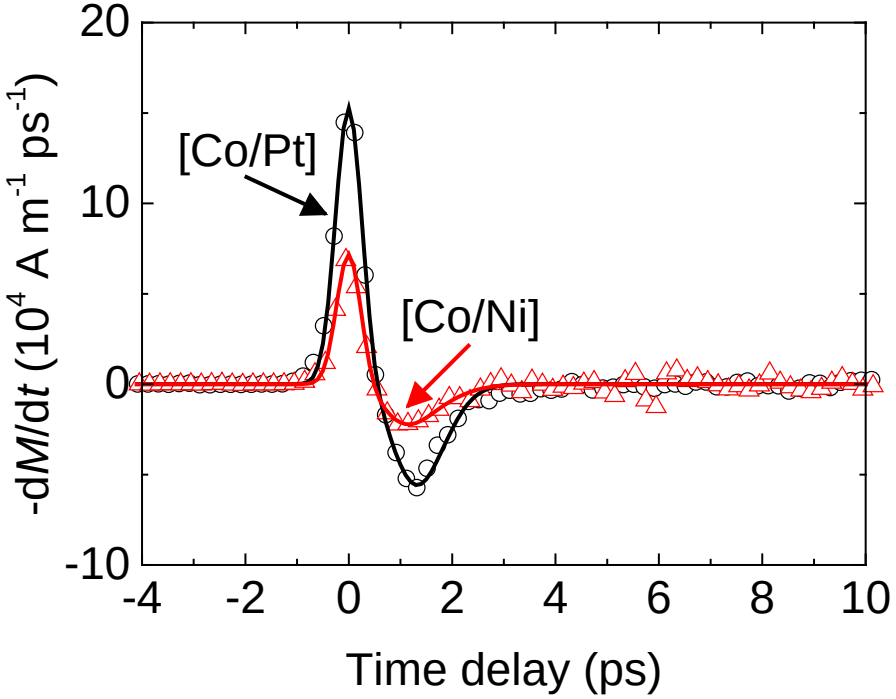

The g_S is obtained from demagnetization data.

The g_S exists only for ~3 ps.

Spin-dependent Seebeck effect (interfacial spin generation) during the time that a temperature gradient exists in the multilayer

Temperature measurement

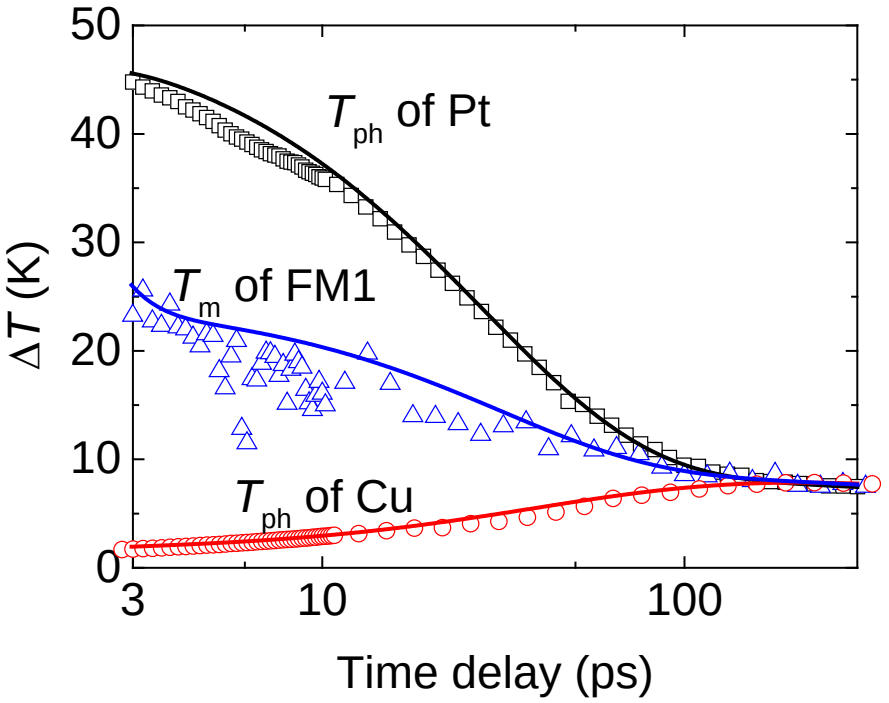

Heat current through FM1

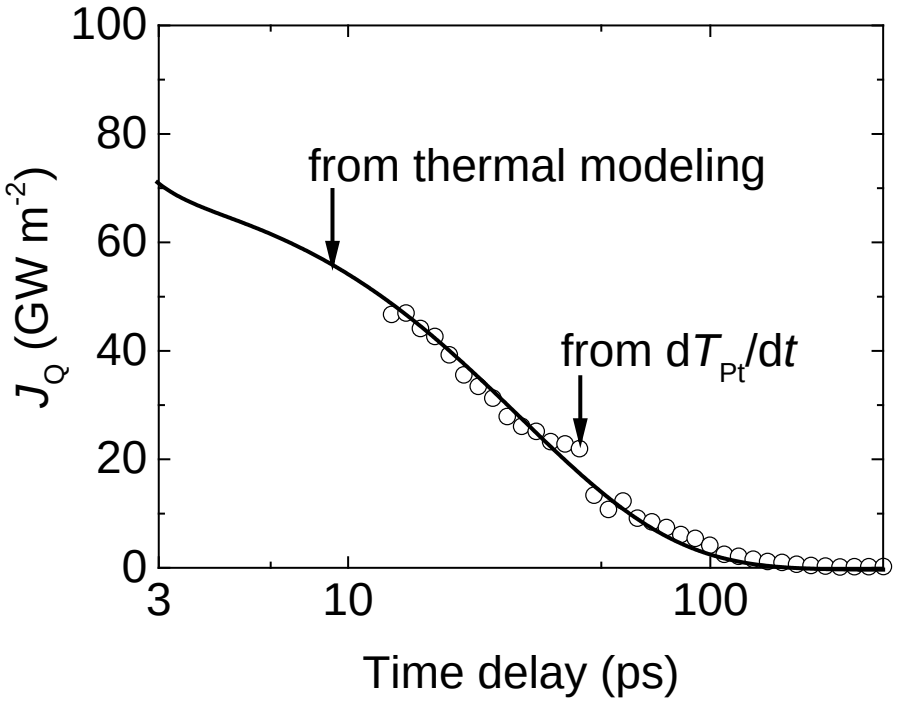

The J_Q is obtained from temperature measurement.

The J_Q persists for ~100 ps.

Use the magnetization dynamics of FM2 to detect the spin current

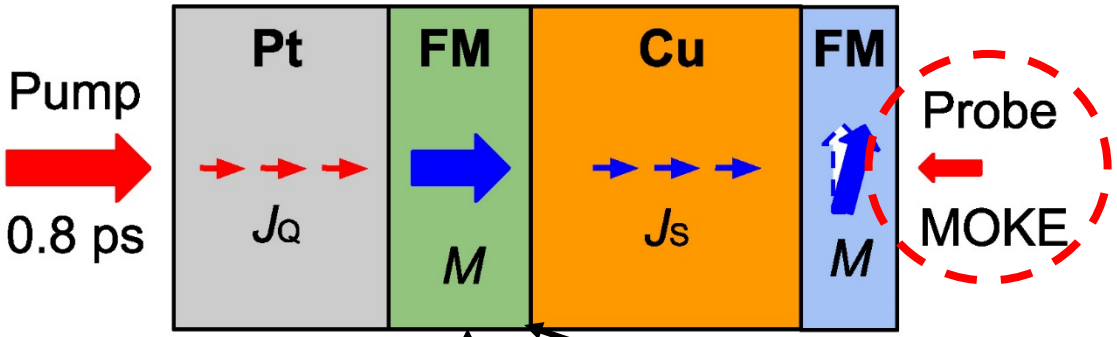

measure M(t) of FM2 with B_X of 0.05 T.

$$g_S = -\frac{dM}{dt} \qquad G_S = -\left(\frac{\mu_B}{eLT}\right) S_s J_Q$$

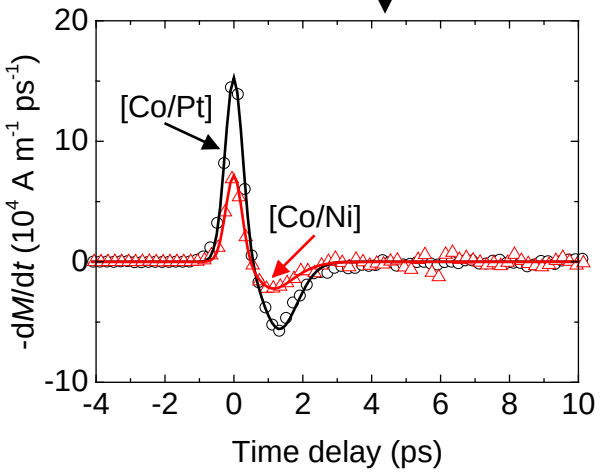

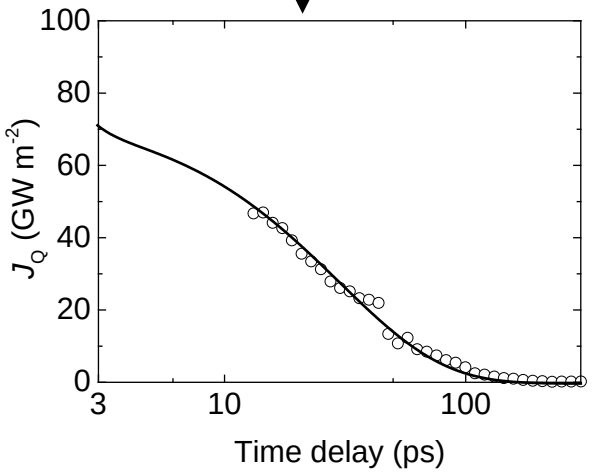

Model by solving the spin diffusion equation

$$\frac{\partial \mu_S}{\partial t} = D\frac{\partial^2 \mu_S}{\partial^2 z} - \frac{\mu_S}{\tau_S} + (\text{spin generation term})$$

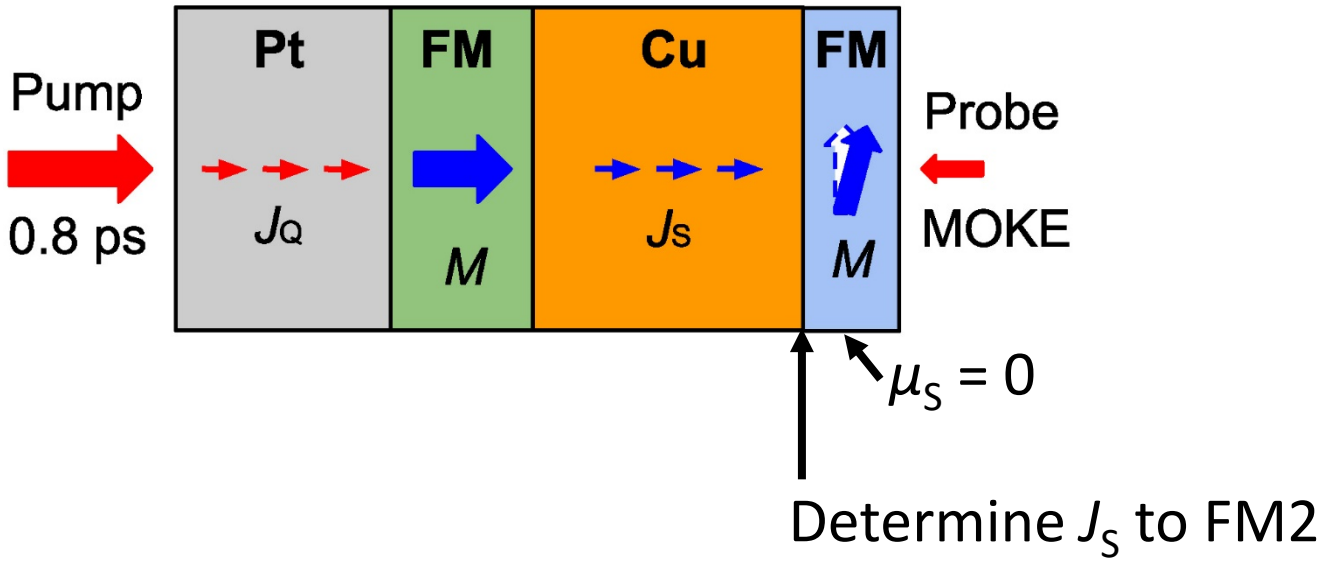

Fitting parameters: τ_S and S_S of [Co/Pt] and [Co/Ni].

Two free parameters: spin relaxation time and spin-dependent Seebeck coefficient

$$\dot{\mathbf{m}} = -\gamma_e \mathbf{m} \times \mathbf{H}_{\text{eff}} + \alpha \mathbf{m} \times \dot{\mathbf{m}} + \frac{J_S}{M_S h} \mathbf{m} \times (\mathbf{m} \times \mathbf{m}_{\text{fixed}})$$

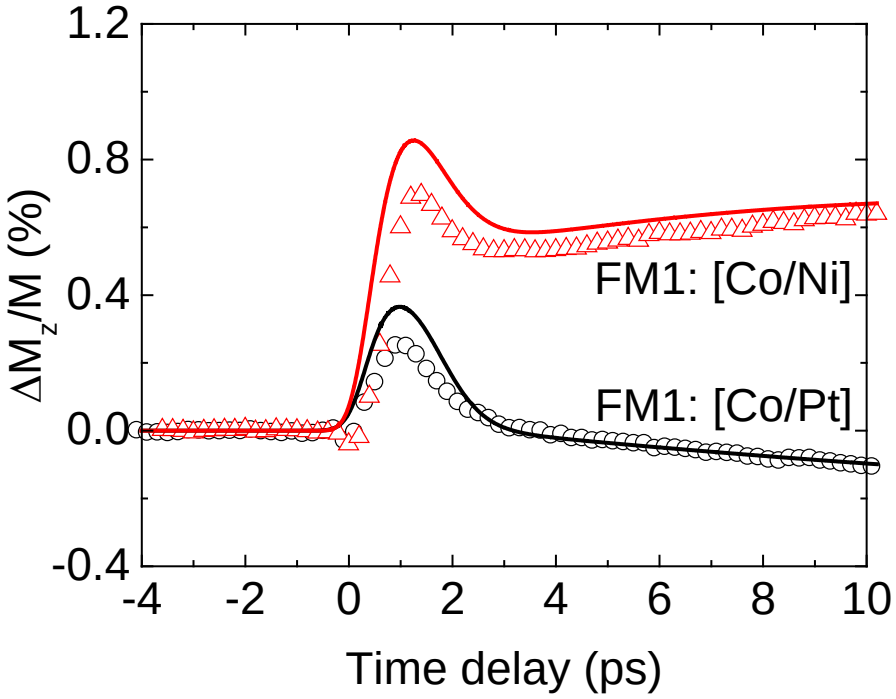

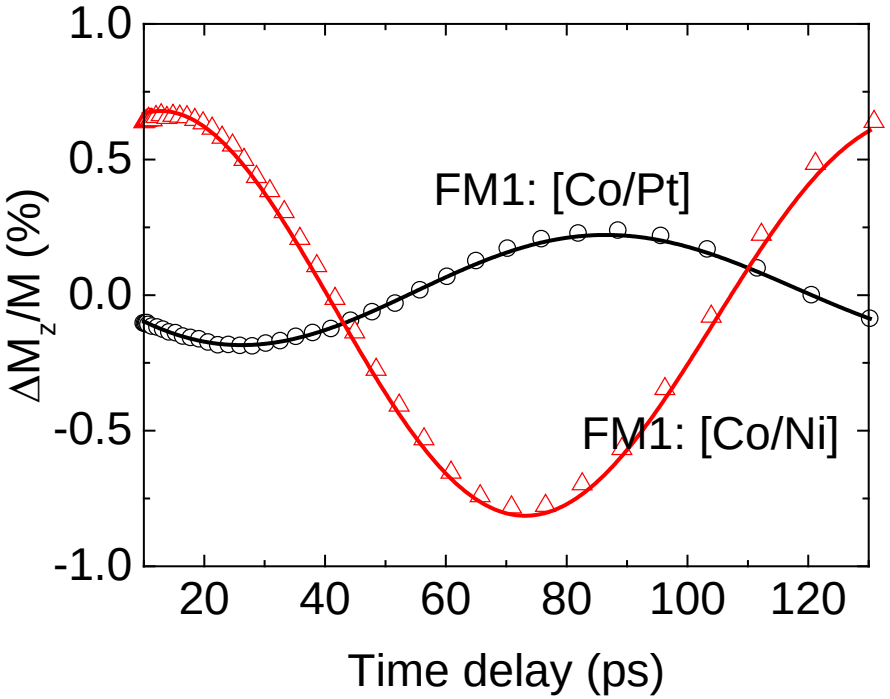

Fitting results	[Co/Pt]	[Co/Ni]
τ_S	0.02 ps	0.1 ps
S_S	6 μV/K	-12 μV/K

Final topic: Ultrafast thermometry with nanodisk plasmonic sensors

- Fabricated by “hole-mask colloidal lithography”

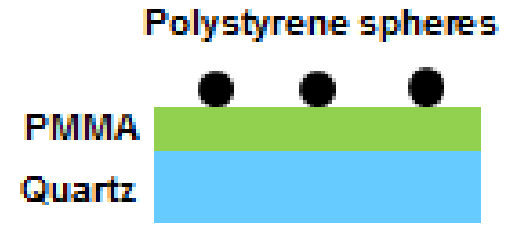

1) Spin-coating of resist and dispersion of spheres on top

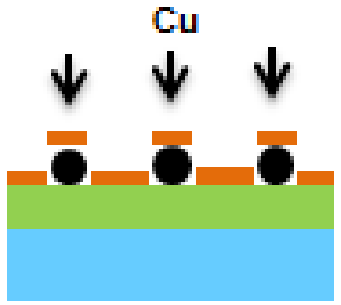

2) Evaporation of metal mask

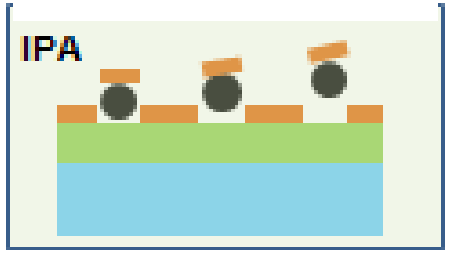

3) Stripping off the spheres by sonication in IPA

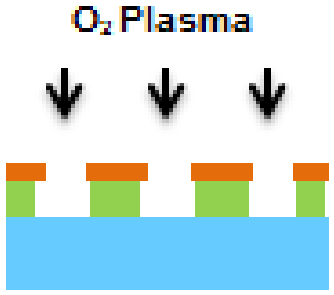

4) Oxygen plasma etching

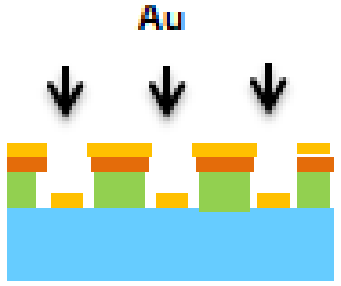

5) Au deposition

6) Lift-off

Nanodisk plasmonic sensors

- SEM gives the most accurate measurement of diameter
- AFM gives the most accurate measurement of height

Au disk diameter 120 ± 10 nm, height 20 ± 2 nm

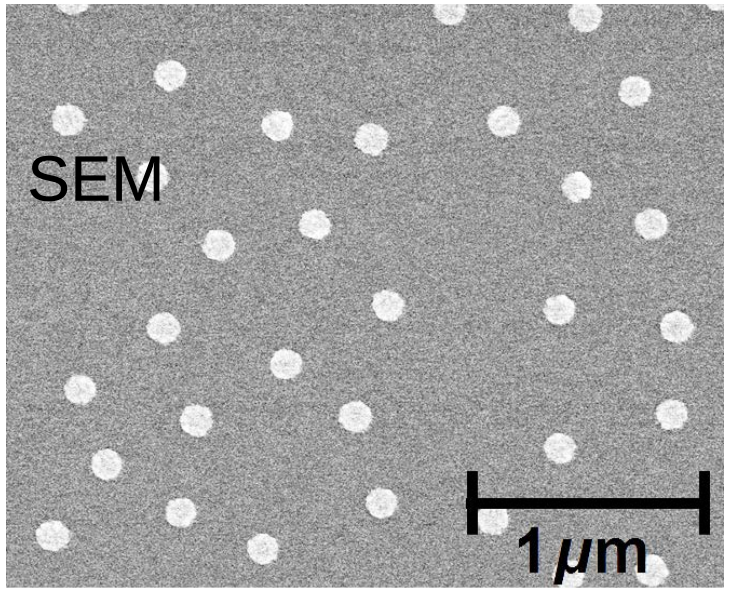

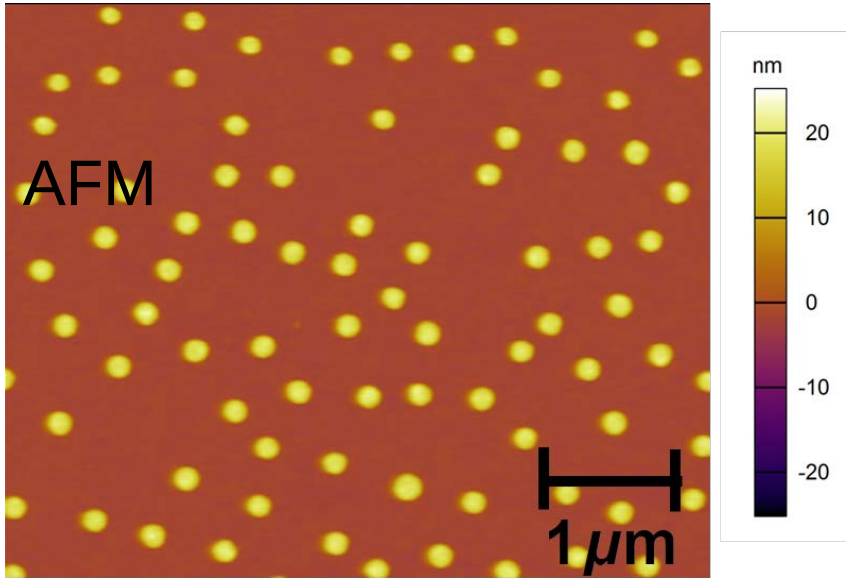

Park and Cahill, J. Phys. Chem. C (2016)

Sensitivity *d(Tr)/dn* (change in transmission coefficient with respect to optical index) approaches unity

- Coat with PMMA and take difference spectra of the absorption.
- Noise floor of pump-probe measurements is

$$\Delta n \approx 0.3 \text{ ppm Hz}^{1/2}$$

$$\Delta T_{liquid} \approx 3 \text{ mK Hz}^{1/2}$$

$$\Delta h_{liquid} \approx 10^{-13} \text{ m Hz}^{1/2}$$

Tr = transmission

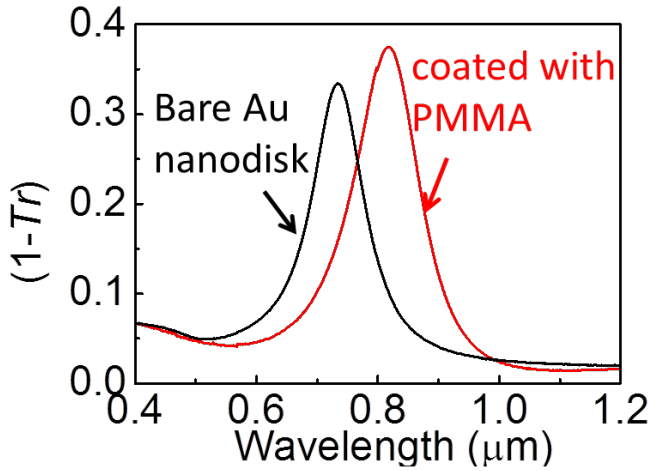

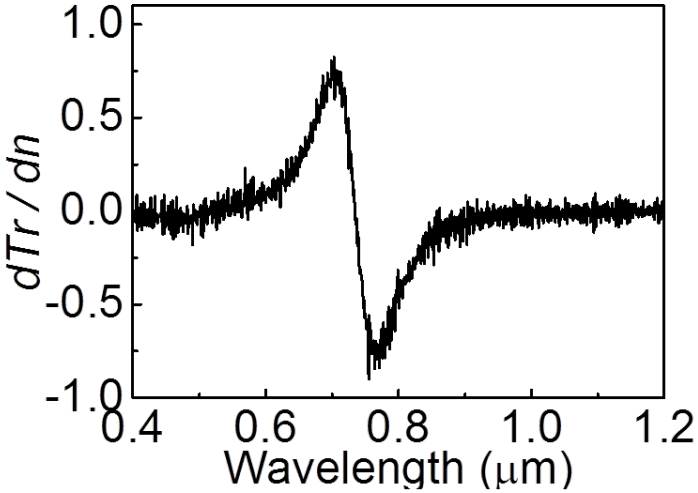

Sensitivity to *dn* is localized to within 13 nm of the Au surface

- Atomic-layer deposition of alumina
- Alumina thickness on planar Au surface measured by ellipsometry.

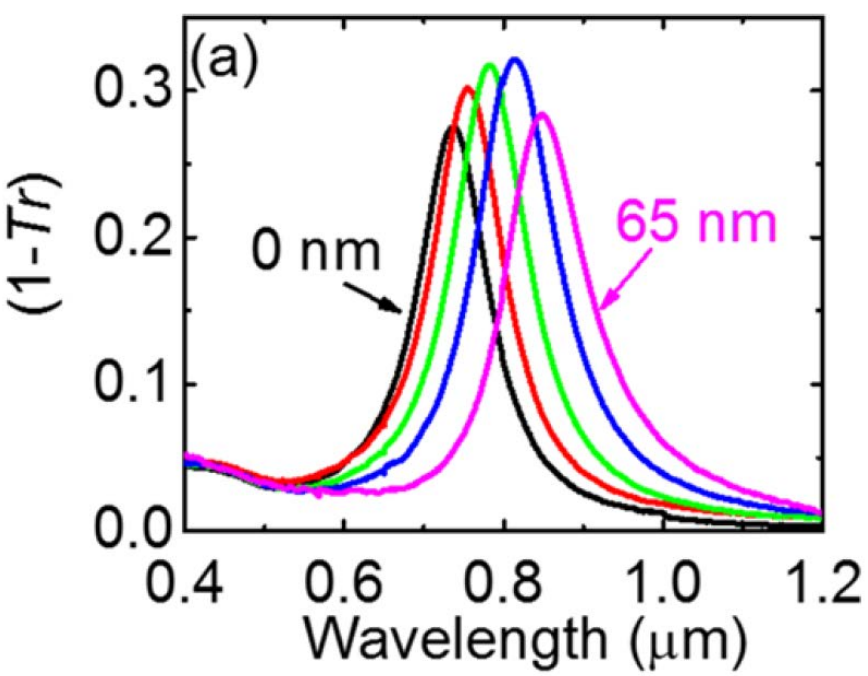

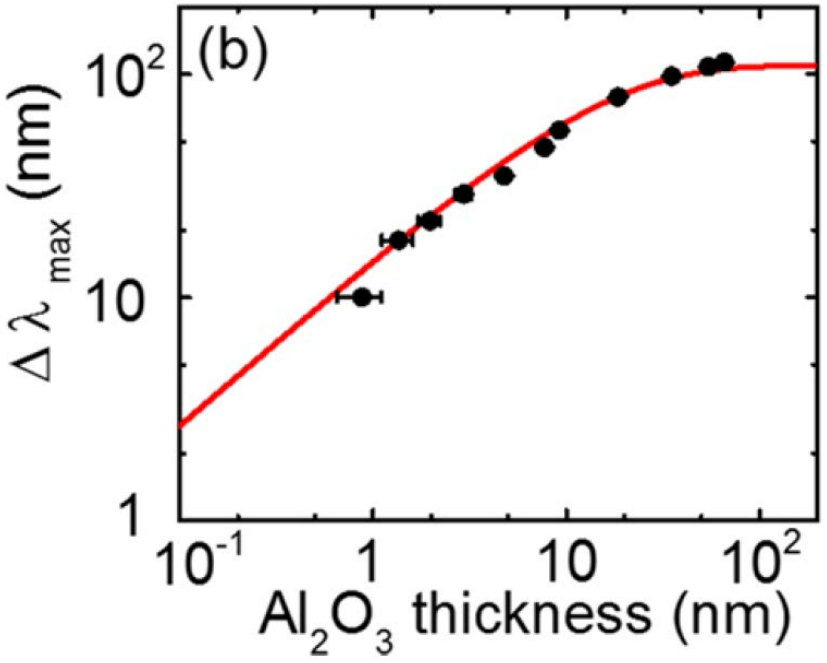

Transient absorption

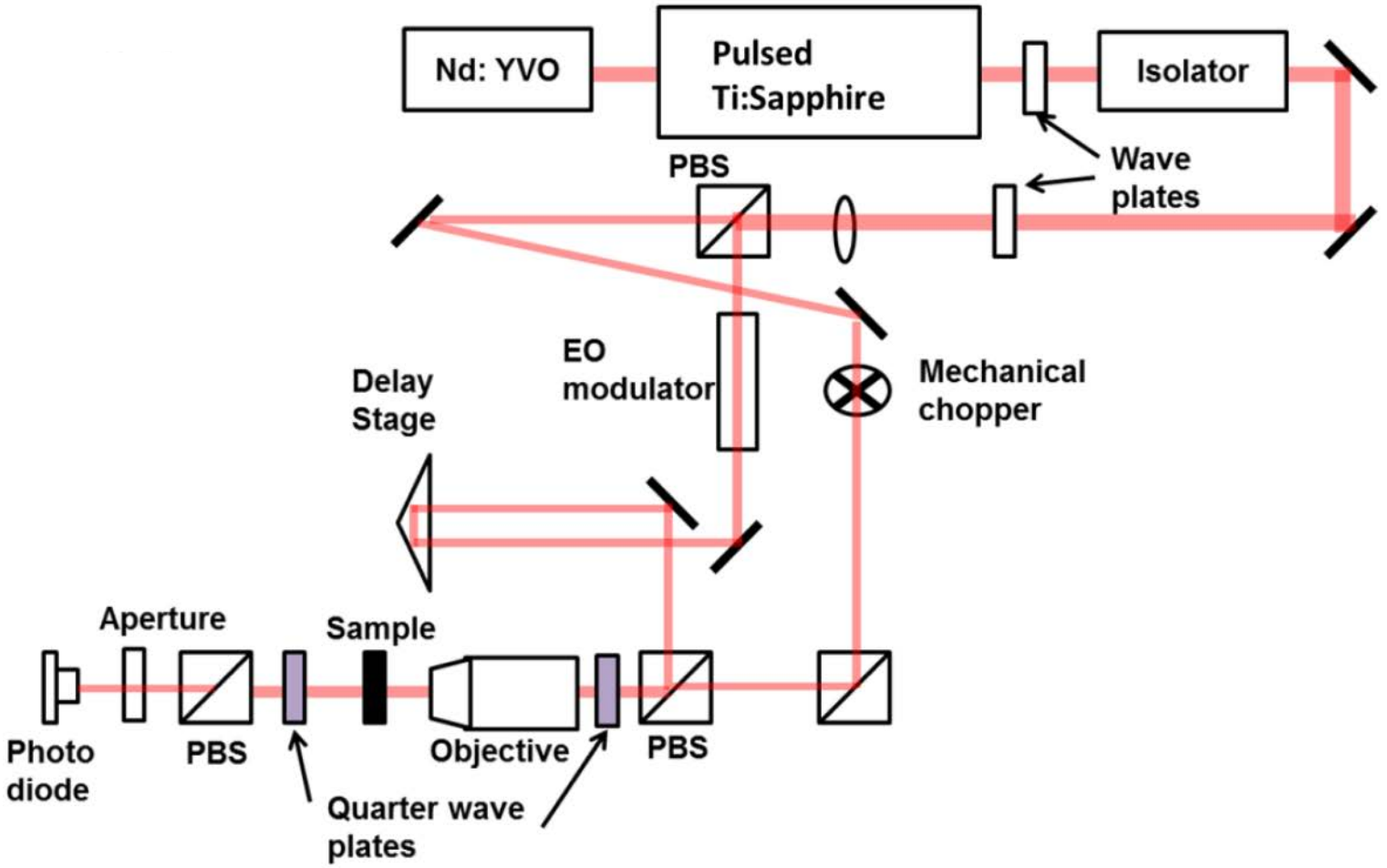

Signal is a combination of the temperature change of the Au and the temperature change of the surroundings

$$\Delta Tr = \frac{d(Tr)}{dT_{Au}}\Delta T_{Au} + \frac{d(Tr)}{dT_{fluid}}\Delta T_{fluid}$$

- Isolate the two terms using a linear combination of the response at two wavelengths.

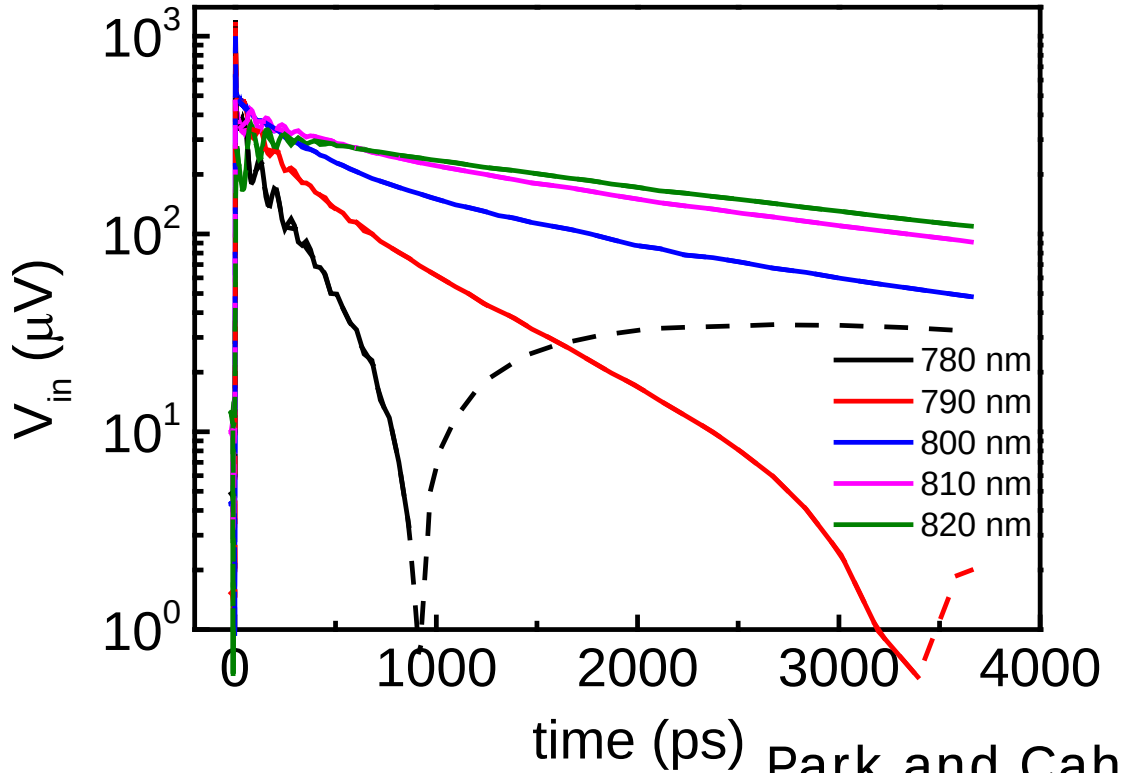

see also: Stoll, Vallée *et al.*, JPCC (2015)

Park and Cahill, J. Phys. Chem. C (2016)

Signal from the lateral “breathing mode” acoustic oscillation is minimized at the same wavelength that minimizes the sensitivity to fluid temperature

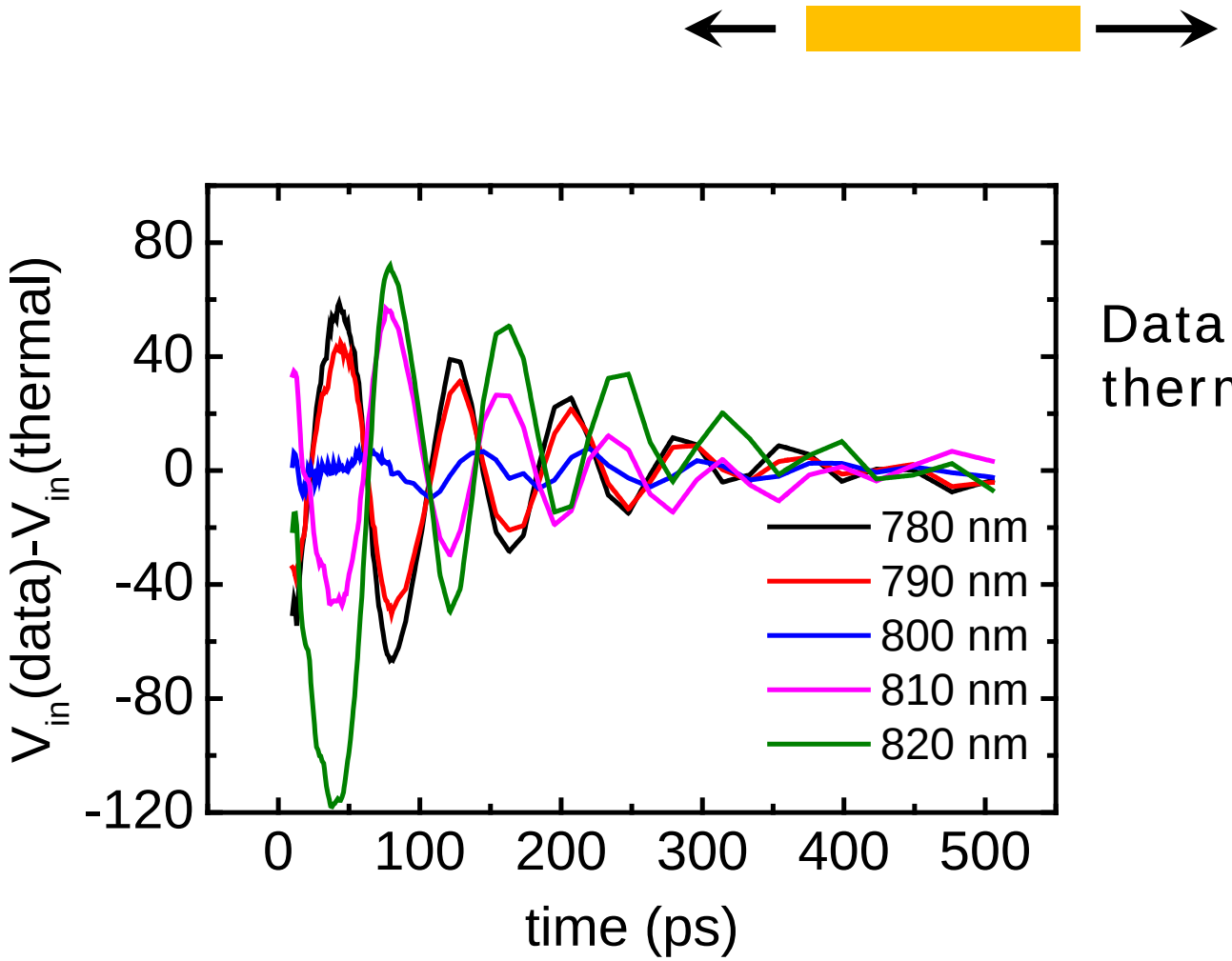

Data after subtracting thermal response

Numerical modeling of the temperature field

- dn/dT of the fluid dominates over dn/dT of the glass substrate so model the signal as a weighted average of the temperature of the fluid within (13 nm)*(n_{Al2O3}/n_{liquid}) of the Au nanodisk
- Au/silica interface conductance from an independent measurement.

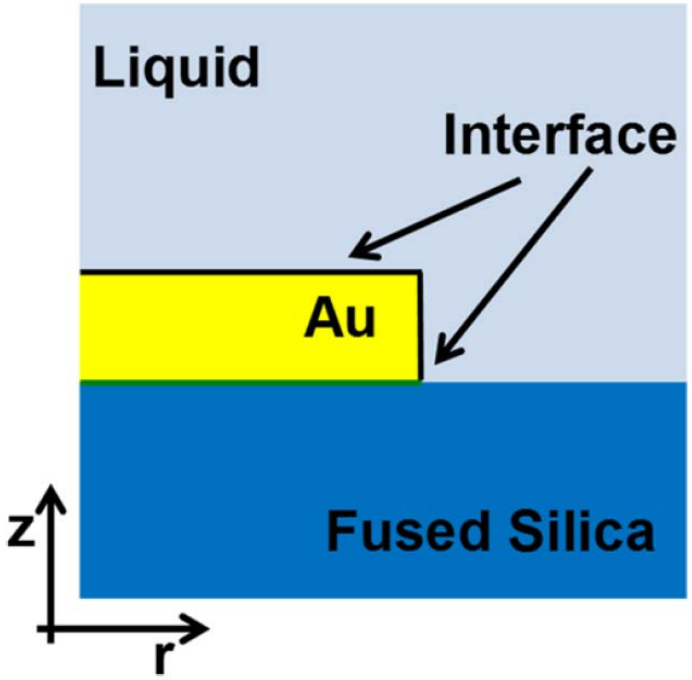

Park and Cahill, J. Phys. Chem. C (2016)

Data analysis and sensitivities for interfaces with fluid mixtures

- Control surface chemistry with self-assembled monolayers: hydrophilic $HS(CH_2)_3SO_3$ and hydrophobic $HS(CH_2)_9CH_3$.
- Subtract breathing mode acoustic signal by fitting to a damped oscillator
- Compare to thermal model with interface conductance as a free parameter

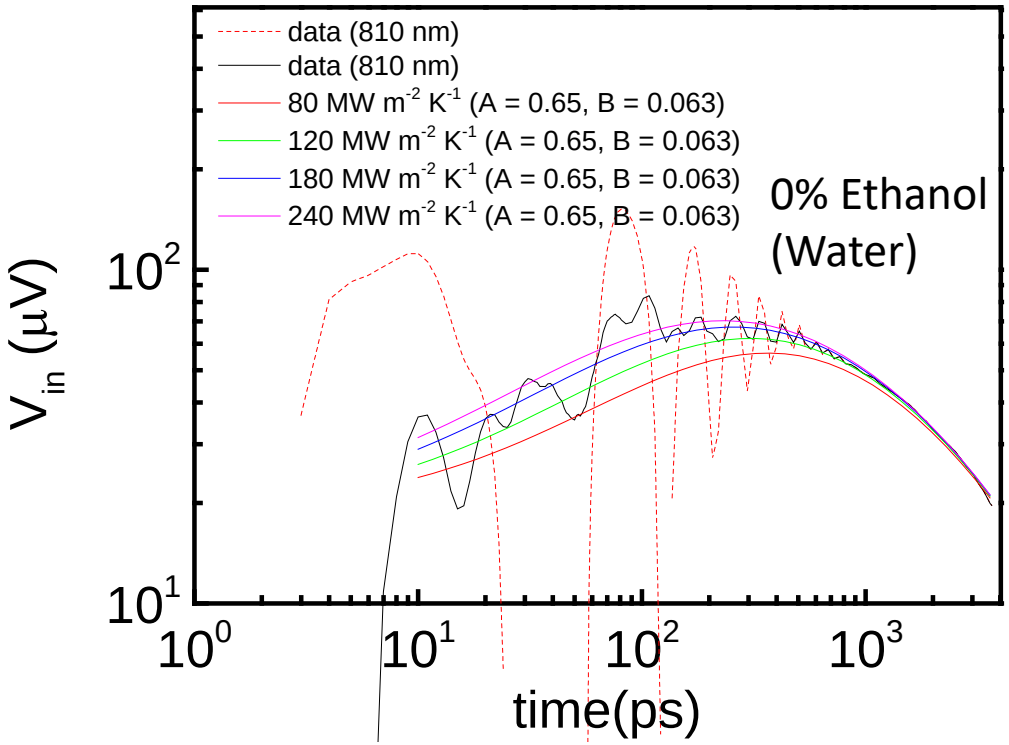

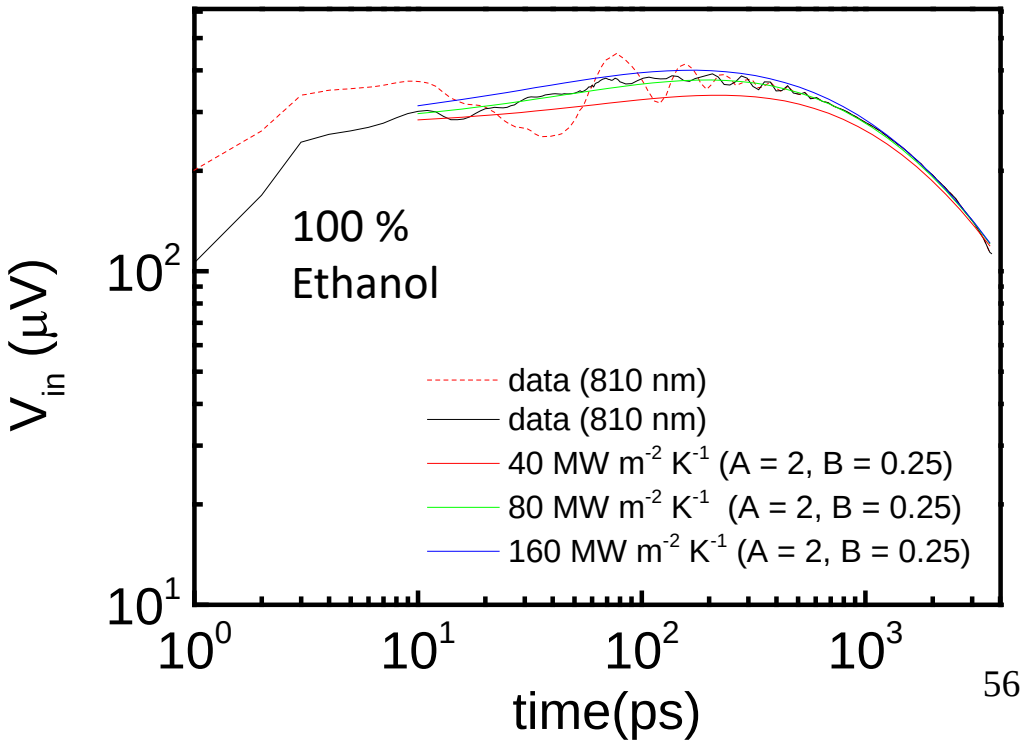

Vary liquid composition between pure water and pure ethanol for hydrophobic SAM, hydrophilic SAM, and “bare” Au

- Data for pure water and pure ethanol are in agreement with prior work for planar interfaces and supported nanoparticles.
- Data for pure ethanol are relatively insensitive to the interface chemistry.

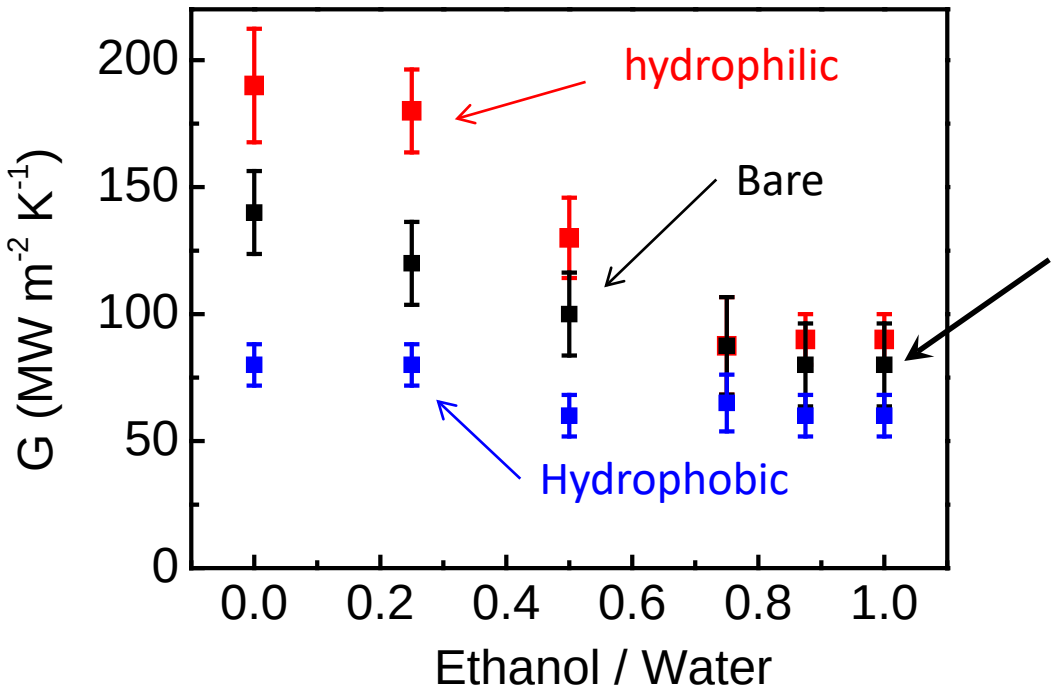

Kapitza length

$L_K = \Lambda/G \approx 3$ nm

Park and Cahill, J. Phys. Chem. C (2016)

Summary of time-domain thermoreflectance

- Time domain thermoreflectance (TDTR) is a robust and routine method for measuring the thermal conductivity of almost anything (that has a smooth surface).
- Data—and uncertainties in the data—can be analyzed rigorously as long as the diffusion equation is a valid description of the heat conduction.
- Noise floor of the temperature measurement is on the order of 5 mK $Hz^{-1/2}$
- Sensitivity to heat transport at short times is typically limited to ~300 ps by the thermal mass of the metal film transducer.

Summary of magnetic and plasmonic ultrafast optical thermometers

- Kerr effect transducers are relatively immune to what is happening in other parts of the sample. Polarization rotation is specific to the magnetic layer.
  - Thin transducers enable higher time resolution and better sensitivity in many experiments
  - Enables ultrafast measurements of magnetic and electronic temperature
  - Noise floor is comparable to TDTR, 5 mK $Hz^{-1/2}$
- Time-resolved magnetic birefringence can probe magnetic temperature of antiferromagnets
- Plasmonic sensors can be used to determine the temperature field in a transparent material adjacent to the sensor.
  - High sensitivity to temperature (3 mK $Hz^{-1/2}$) or thickness of adsorbed layers (0.1 pm $Hz^{-1/2}$)